Mauro Filipe Ramalho da Costa

Bachelor in Sciences of Physics Engineering

Decontamination and deodorization of 2,4,6-trichloroanisole on cork

Dissertation submitted in partial fulfillment
of the requirements for the degree of

Master of Science in
Physics Engineering

Adviser: Orlando M. N. D. Teodoro, Professor,
Faculty of Sciences and Technology, NOVA University of Lisbon

FACULDADE DE
CIÊNCIAS E TECNOLOGIA
UNIVERSIDADE NOVA DE LISBOA

September, 2017

Decontamination and deodorization of 2,4,6-trichloroanisole on cork

This document was created using the (pdf)LaTeX processor, based in the "novathesis" template[1], developed at the Dep. Informática of FCT-NOVA [2].
[1] https://github.com/joaomlourenco/novathesis [2] http://www.di.fct.unl.pt

"I would rather have questions that can't be answered than answers that can't be questioned."
— Richard Feynman

Acknowledgements

First of all i would like to thank to the Faculty of Sciences and Technology of the NOVA University of Lisbon (FCT-UNL) for having been a place that I could call home throughout the five years of this course.

I would also like to thank to the following persons for all the teachings and support offered:

Professor Orlando, for accepting to be my adviser and for all the teachings and patience, not only in this master's thesis but also throughout the many disciplines in the course where we have met.

Nenad, for always being so receptive and for always having a suggestion regarding the many phases of our work.

Afonso and Ana for being so supportive and helpful with the technical work in Metrovac and for always being in a good mood.

Professor Jorge Silva and Professor Célia Henriques for being so helpful and for lending us several materials and equipment in many of our work phases.

Professor Moutinho for his enthusiasm and curiosity in our work.

Mr. Faustino and Mr. Mesquita for lending us their workshops whenever it was needed.

My parents for doing the impossible so I could be finishing this same sentence.

All my friends for still being my friends after I had to skip many dinners.

And at last but not the least, a special thanks to Carolina for always being so supportive, for all the help and patience during this course and surely I will not forget what the Auger effect is.

Abstract

The presence of 2,4,6-trichloroanisole (2,4,6-TCA) in cork was identified as a problem for the cork industry in the early 80's and also considered as a potent compound towards the origin of organoleptic defects in wines. These defects are easily detected by the consumers and it only takes as little as about 5 ng/L to be detected. However, there is a certain difficulty when trying to detect such low concentration levels with mass spectrometry. Heavily contaminating the cork substrates with TCA could be a solution for this detection limitation.

By artificially contaminating the samples and by using quadrupole mass spectrometry (QMS) coupled with temperature-programmed desorption (TPD), we verified the presence of a TCA desorption peak in a cork substrate. We also verified that heating above a temperature of 160ºC in a high vacuum atmosphere allows the removal of this contaminant from cork substrates. A TCA quantification method that was developed with this work confirmed that the majority of the TCA was removed with the TPD experiment when heating above the TPD peak.

The main outcome of this experiment is the proposed process to remove TCA from cork stoppers by heating at temperatures close or above the TPD peak. Such process would have the goal of making cork and its derivative products free of TCA, or at least below the human detection threshold. In order to achieve this goal, it is necessary to understand how the TCA adsorption occurs, and that will be the objective and the contribution of this thesis work - to confirm the nature of the TCA adsorption and, most importantly, an attempt to determine which group of its molecule is effectively adsorbing onto the cork substrates. For this purpose, other substrates and compounds were chosen to be experimented due to their similarities with the constitution of cork constitution and the chemical structure of TCA, respectively. This experiment showed that cellulose does not have a relevant role in the adsorption process.

Keywords: Cork, Trichloroanisole, Adsorption, Temperature-Programmed Desorption, Quadrupole Mass Spectrometry.

Resumo

A presença de tricloroanisol (2,4,6-TCA) em cortiça foi identificada como um problema para a indústria corticeira no início dos anos 80 e foi também considerado um potencial composto na origem de defeitos organolépticos em vinhos. Esses defeitos são facilmente detectáveis pelos consumidores sendo a sua detecção possível com uma concentração de apenas 5 ng/L. No entanto, existe uma certa dificuldade na detecção destes niveis de concentração utilizando espectrometria de massa. Uma forte contaminação nos substratos de cortiça com TCA poderá ser uma solução para esta limitação na detecção.

Ao contaminar amostras artificialmente e usando espectrometria de massa do tipo quadrupolo (QMS) juntamente com desorção a temperatura controlada (TPD), verificou-se a presença de um máximo de desorção de TCA num substrato de cortiça. Também se verificou que o processo de aquecimento a temperaturas superiores a 160ºC é capaz de remover TCA do substrato de cortiça quando em alto vácuo. Um método de quantificação de TCA, desenvolvido com este trabalho confirmou que a maioria de TCA era removido com um processo TPD, quando aquecido a temperaturas acima do pico detectado.

Com este resultado experimental é possível propor um processo de remoção de TCA das rolhas de cortiça aquecendo-a temperaturas próximas ou superiores do pico TPD. Tal processo teria a finalidade de remover o TCA da cortiça e dos seus derivados, pelo menos de forma a que este composto não seja detectável. Por forma a atingir este objetivo, é necessário compreender de que modo a adsorção de TCA ocorre, sendo esse o principal objectivo e contribuição desta tese - confirmar a natureza da adsorção do TCA e, mais importante, uma tentantiva de determinar qual o grupo desta molécula que efectivamente se liga aos substrato de cortiça. Para esta finalidade, outros substratos e compostos foram escolhidos para serem testados, devido às suas semelhanças com a constituição da cortiça e da estrutura química do TCA. Com este ensaio verificou-se que a celulose não tem um papel relevante na adsorção.

Palavras-chave: Cortiça, Tricloroanisol, Adsorção, Dessorção a Temperatura Controlada, Espectrometria de Massa do tipo Quadrupolo.

Contents

List of Figures

List of Tables

List of Symbols

τ	Monolayer formation time
λ	Free mean path
α, β	Heating Rate
ν_n	Pre-exponential factor
A	Aperture Section
C_{He}	Conductance for helium
C_{TCA}	Conductance for TCA
D	Diameter of the restriction
E_{act}	Activation Energy
E_{des}	Desorption Energy
E_{dis}	Dissociation Energy
Kn	Knudsen number
M	Molar mass of the solid material
M_{He}	Molar mass of helium
M_{TCA}	Molar mass of TCA
P	Pressure
P_{He}	Partial pressure of helium
Q_{He}	Throughput of helium
$Q_{He,Ref}$	Throughput of helium from the reference leak
$Q_{TCA,Ref}$	Throughput of TCA from the reference leak
$Q_{TCA,unk}$	Throughput of TCA from the contaminated substrates
R	Ideal gas constant
$Signal_{He}$	Signal of helium measured
$Signal_{He,Ref}$	Signal of helium measured from the reference leak
T	Temperature
T_0	Initial temperature
T_p	Temperature at which the peak's maximum occurs
k_n	Rate constant
n_m	Number of particles in a monolayer per cm^2

r_{des}	Rate of desorption
t	Time

List of Acronyms

EGA	Evolved-gas analysis
GC-MS	Gas Chromatography-Mass Spectrometry
IL-SDME	Ionic liquid-based single drop microextraction
IMS	Ion mobility spectrometry
PID	Proportional-integrative-derivative
QMS	Quadrupole mass spectrometry
SBSE	Stir bar sorptive extraction
SFE	Supercritical fluid extraction
SPME	Solid-Phase Microextraction
TBA	2,4,6-tribromoanisole
TBP	2,4,6-tribromophenol
TCA	2,4,6-trichloroanisole
TCB	1,3,5-trichlorobenzene
TCP	2,3,4,6-tetrachlorophenol
TDS	Thermal desorption spectroscopy

TPD	Temperature-programmed desorption
UHV	Ultra-high vacuum
USAEME	Ultrasound-assisted emulsification extraction

Chapter 1

Introduction

A general introduction to the topic of this thesis is done in this chapter. The contextualization and the source of the problem is described and discussed. It is also mentioned the background related to this field and how it contributed with different aspects. In the end of this chapter there is an introduction to our contribution on this subject and what are the intended goals.

1.1 Contextualization

Portugal is the main producer of cork in the world. This requires special concerns towards the quality of cork. Regarding its different applications, different tests have to be done in order to guarantee the quality of the cork.

We will focus on one of the main usages of the cork - cork stoppers. This piece of refined cork serves the purpose of containing and preserving the state of certain beverages, typically wine, thus the cork stopper should not have releasable contaminants that would degrade its state.

Wine producers typically use cork stoppers. However for a few years, some producers stopped using cork as the preferred material for stoppers and searched for other solutions such as synthetic stoppers. This was due to the contamination of wine leading to the well-known *cork taint* on wines. It was later determined that this organoleptic defect was mainly caused by 2,4,6-trichloroanisole (TCA) presence on the cork [1].

TCA has a mouldy and earthy odour that lowers the organoleptic quality of the wine. Since it affects the quality of wine, the wine sector was not so receptive towards acquiring more cork stoppers and therefore the cork industry had it's market share lowered. In order to overcome this problem, a huge effort is being made by the cork producers.

It was proven that cork stoppers can be excellent barriers to the transmission of off-flavours from external sources [2]. In the work of Capone et al. they used closed wine bottles and verified that after contaminating the exterior surface of a cork stopper with deuterium labelled TCA, it would not contaminate the wine and most of it stayed in the outer part of the cork even after three years of bottle storage. This means that the cork would only contaminate with TCA if the cork's contamination happened prior to the bottle closure [2]. They also pointed that while observing the slow passage of TCA through the length of the cork supported the argument that the contamination only takes place if the contaminated regions get in direct contact or close enough to the wine.

1.2 Field contributions

The different approaches to this subject are grouped in this section by the different aspects on which they contributed:

- Quality Control
- Detection methods
- Degradation or removal of contaminants

In order to properly understand the detection values in this section, an important term must be introduced and discussed. This term is *releasable TCA* and defines the amount of TCA in a soak when in equilibrium with a given piece of cork, meaning that there is no migration of this off-flavour from the cork to the soak nor the opposite. Hervé et al., that applied the releasable TCA concept as a quality control tool on natural corks, observed that it seems to take approximately 24 hours to reach a TCA equilibrium with the whole piece of cork soaked [3].

The soak consists of a solution of ethanol with water and it is often prepared with the purpose of recreating ethanol concentrations in wines, which should be approximately 90% water and 10% ethanol.

Thus, whenever referring to a detection value, for instance the human detection threshold of TCA which is of 5 ng/L, this value indicates that there are 5 ng of TCA in a litre of the soak solution.

Hervé's group also draw more conclusions towards the releasable TCA. They observed that there is a poor correlation between the total amount of TCA present in a cork stopper and the releasable TCA during the soak process.

Besides that, another experiment was done by the same group regarding bottled wine. It consisted on using highly contaminated cork samples (which were tested for releasable TCA) to closure wines that had no background of TCA. These bottles were then stored neck down and tested for TCA periodically. With this experiment, they found that it is possible to predict the concentration of TCA in a bottled wine. This is possible due to the

strong correlation that was observed between the releasable TCA and the TCA found in the bottled wines. However, unlike what happens with the cork soak, which only requires approximately a day to reach equilibrium, in this case it required 14 months [3]. By the end of this experiment, the authors noticed that there was about half of the releasable TCA measured in the beginning of the experiment in the wine.

Another example of a quality control system is given by *Cork Supply* with their *Innocork* system [4]. It consists of a chamber where the natural cork stoppers are inserted. These samples receive an influx of compressed air which carries both water vapour and ethanol towards the chamber. The gas flux is under controlled temperature conditions. This process allows TCA to be extracted from the cork and along with the compressed air flux prevents re-adsorption onto the cork. Then, taking into account the removed TCA and other odours, they control which samples have the proper quality to hit the market [4].

As far as detection methods are concerned, different approaches are here described.

The group of Evans et. al described and used Solid-Phase Microextraction (SPME) coupled with Gas Chromatography-Mass Spectrometry (GC-MS) in order to analyse TCA in wines [5]. This method required no solvents and the sampling procedure was automated. It was also possible to quantify the analysed TCA down to 5 ng/L. The process had yet to be applied to different cork-related compounds, which may contribute to the unpleasant cork-taint.

Seven years later, in 2004, Z. Penton lowered the detection limit to under 1 ng/L using SPME coupled with GC-MS as well but with different equipments [6].

In 2011, Marquez-Sillero et al. combined Ionic liquid-based single drop microextraction (IL-SDME) with Ion mobility spectrometry (IMS) in order to detect TCA both in water and wine samples. The limit of detection was set in between 0.2 ng/L and 0.6 ng/L. With this experiment they also corroborated that the cork stoppers were the source of the contamination in the wine samples since only those that had the stoppers were contaminated [7].

The group of Fontana et al. proposed an extraction method of TCA from wine samples. It consisted of Ultrasound-assisted emulsification extraction (USAEME) and combined with GC-MS was able to reach detection limits of 0.6 ng/L, also allowing quantitative extractions [8].

Another approach was done by Horst R. in which he explains what lead him to abandon one methodology of work for another. He felt the need to drop SPME for Stir bar sorptive extraction (SBSE) in order to improve the limits of detection (from 2.9 ng/L to 0.3 ng/L) and to increase its productivity, since it allowed to process multiple samples. These methods were always combined with GC-MS.

There was also developed a cellular biosensor in order to detect TCA. It detected TCA in cork soaks in about 3 to 5 minutes covering the whole range of human detection [9].

In May 2016, Amorim Cork announced that their quality control system is able to guarantee and deliver cork stoppers that no longer cause the cork taint [10]. Using a sophisticated and fast GC-MS technique, they affirm that they are able to detect an individual contaminated cork stopper with more than 0.5 ng/L in just a matter of seconds allowing the technology to be adapted on an industrial scale. However, the cork stoppers identified as being above the TCA threshold defined by Amorim Cork, are removed from the usable lot.

Cork treatment and removal or degradation methods were also proposed.

In 2000, Taylor et. al developed a Supercritical fluid extraction (SFE) method which was then combined with GC-MS with selected ion monitoring to allow quantification of the removed TCA from cork stoppers [11].

An attempt on trying to remove taste and odour of TCA from water by using tight ultrafiltration membranes was done by Park et al. In their work they noticed that their main concern was the TCA adsorption on the membranes surface [12].

The patent FR2884750(A1) uses a set-up that has the intended goal of lowering the partial pressure that the released TCA from cork exerts, to a sufficiently low pressure level [13]. This pressure level is not specified in the patent. The system has a mass spectrometer and it may have lamp in order to heat the stoppers. However, in this patent the temperature control is optional and the samples seem to consist of both non-contaminated and contaminated stoppers. It should be noticed that there are no mass spectrometers with enough sensitivity to detect naturally contaminated cork stoppers, which should be a problem in this patent.

Vlachos et al. tried to treat cork barks and natural cork stoppers by sterilising them. They used different types of gases in this steralization. Gaseous ozone was used on cork barks while a combination of steam and ozone was used for cork stoppers. Even though ozone was enough to sterilise and conserve the cork bark for a week, it wasn't enough to contribute to the deodorization of cork stoppers [14].

Also Vlachos et al., on a different investigation, tried a degradation of TCA by gas-phase photocatalytic, while in a presence of a nanocrystalline titania film. It was developed in order to treat cork stoppers. The photodegradation was obtained while using black light tubes of low intensity emitting near-UV, meaning that the solar light could also be used for this degradation [15].

Another degradation experiments were realized. Back in 2001, Careri et al. irradiated TCA with an electron beam and analyses were done with the GC-MS technique. This irradiation caused the degradation of TCA into different compounds such as 2-chloroanisole, 4-chloroanisole, 2,4-dichloroanisole and 2,6-tricloroanisole. Quantitative data showed that with the increase of the radiation dose, the TCA amount decreased while the concentration of its derivatives, except 2,6-trichloroanisole, increased [16].

Besides the degradation already mentioned, there was also proposed a degradation method by gamma-rays. The experiment demonstrated that it is possible to transform

the TCA present in contaminated cork stoppers by using gamma-rays. This contributes to the reduction of the sensory defects since it creates molecular residues which do not have odour characteristics [17].

1.3 Understanding TCA adsorption in cork substrates

The molecules of TCA are bound with cork substrates, which means that it should be possible to remove them when given a certain amount of energy. Acknowledging this, it should be possible to observe a manifestation of the removed TCA. This is only observable when combining gas chromatography with mass spectrometry (GC-MS) since the GC technique pre-concentrates the TCA, allowing it to be properly detected by the mass spectrometer. A direct measurement of the desorbed TCA is not possible, if only naturally contaminated cork stoppers are considered.

However, if we artificially contaminate cork substrates with a reasonable amount of TCA and submit them to a given temperature, it should be sufficient to detect the desorbed contaminant by mass spectrometry, when in a vacuum atmosphere.

Combining both temperature programmed desorption with quadrupole mass spectrometry allowed us to observe a TCA desorption peak. This experimental result allowed us to set new objectives.

A long term objective for this work is to design an appropriate system of extraction of TCA or other off-flavours from cork stoppers. However, in order to do so, it is necessary to properly understand the details behind this particular case of adsorption, and that will be our contribution with this work.

Thus, the objectives of this thesis are identifying whether the adsorption is a chemisorption or a physisorption and, most importantly, which group of 2,4,6-TCA molecule is effectively bonding with the cork substrate.

For this purpose, different experiments were conducted. However, the substrate contaminating procedure was kept consistent, meaning that the substrates were always artificially contaminated with the sufficient amount to properly detect the removed TCA.

These experiments consisted on using different adsorbates and substrates, which were chosen regarding both the constitution of cork and the chemical structure of cork, and performing a Temperature-programmed desorption (TPD)) experiment for each combination of adsorbate/substrate. In these series of experiments an answer should be found regarding the bonds of TCA with cork.

Chapter 2

Concepts and experimental techniques

In this chapter the physical phenomenons and experimental techniques that will be more frequently referred throughout this dissertation are discussed. Starting with the phenomenon behind temperature-programmed desorption, adsorption is the first to be described. Later the technique itself will be explained as well as a brief explanation on Quadrupole mass spectrometry (QMS).

2.1 Physical and Chemical Adsorption

There are different types of sorption to be considered. Besides the absorption case, there are two other types of sorption to be explained: physical and chemical adsorption.

Before explaining the adsorption processes, a couple terms have to be introduced. These terms are adsorbate or adparticles and adsorbent material. The adsorbent refers to the solid material where the colliding particles adhere and stick to the material. The particles that adhere or are adsorbed are the adsorbate or adparticles and could either be in a gas phase or liquid phase. Making a brief analogy with the work in this thesis, the adsorbate is TCA, while the adsorbent material is cork, more specifically the substrate's surface.

In figure 2.1 are represented the terms for the elements participating in an adsorption process. The white circles represent atoms in the solid material and the grey circles represent the particles being adsorbed. In it is possible to observe how adsorption occurs. Whenever an incident gas particle collides with the material and enough energy is involved, an adsorption may occur. If it is adsorbed, it stays on the surface of the material until it has enough energy again to be desorbed. This desorption energy can be provided thermally, by heating the surface.

Notice that adsorption should not be mistaken with absorption. Absorption consists

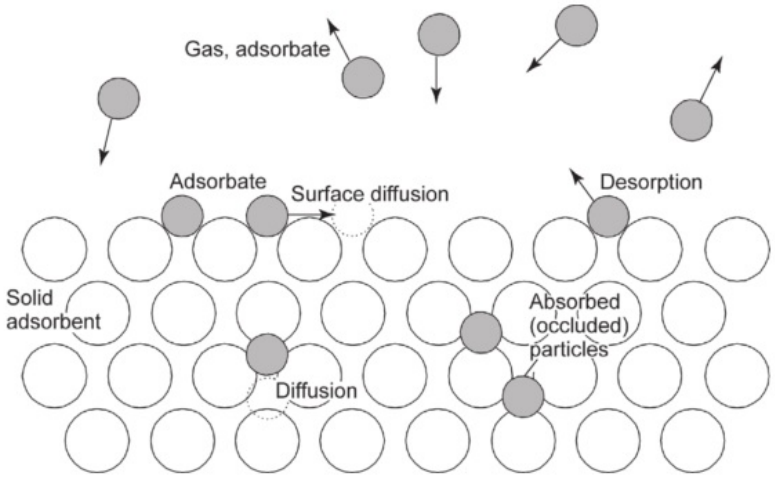

Figure 2.1: Elements and processes involved in adsorption. Image obtained from [18].

on a migration or diffusion of the adparticles into the solid material interstitial sites or lattice defects or even moving along grain boundaries of crystallites [18]. Adsorption consists on a phenomenon that occurs at the surface of a solid material and may be described as when an attractive interaction between a surface and a particle holds enough energy to overcome the effect of the thermal motion [19].

Two other terms that should not be mistaken, even though they are often used in the same context are desorption and outgassing. While desorption occurs in the surface, outgass is the process in which a particle dissolved in a solid has to travel to the surface and then desorb [18].

There are two categories of adsorption, physical and chemical adsorption:

- Physical adsorption relies essentially on van der Waals forces or dipole forces to stablish the physisorption and are typically characterised by dissociation energies below 50 kJ/mol [18, 19];

- Chemical adsorption or chemisorption estabilishes an atomic bonding and its dissociation energies are usually above the 50 kJ/mol. It occurs whenever the overlap of the molecular orbitals of the adsorbed particle and the surface atoms allow the formation of a chemical bond [18, 19].

In the following figure 2.2, both physisorption and chemisorption phenomenons are indicated regarding on how the potential energy develops with the increase of the distance from the solid material's surface. Depending on the curve, this potential is either regarding a diatomic molecule A_2, or two atoms 2A.

Considering the molecule curve we notice that a potential well takes shape between 0.2 nm and 0.4 nm. Furthermore, if the molecule A_2 would be adsorbed, its adsorption would hold energy equal to E_p.

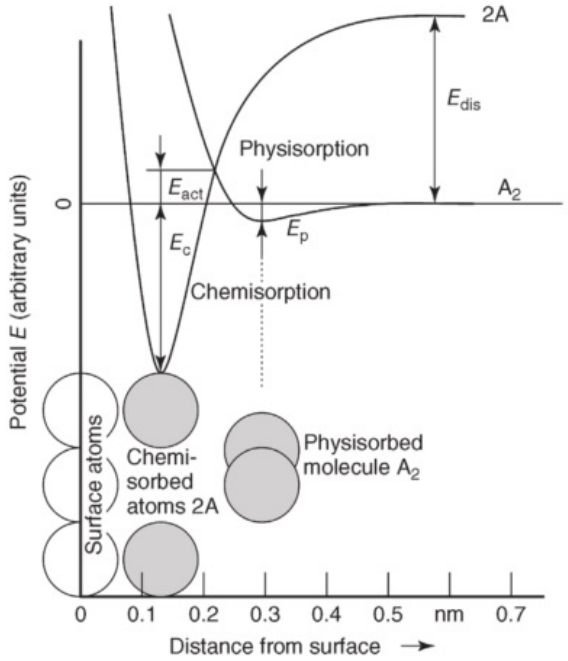

Figure 2.2: Lennard-Jones potential for a certain physisorption and chemisorption process. Image obtained from [18].

The energy E_{dis} is considered when dissociating the molecule A_2 into two atoms. For instance if the molecule A_2, approaching the surface, receives enough energy to overcome E_{dis} at a distance above 0.6 nm, it would dissociate and could possibly lead to chemisorption. However, near the surface it would be easier to dissociate this molecule by only overcoming the activation energy E_{act} instead of the previous E_{dis}. After dissociation, chemisorption can take place and adsorb both atoms A at a distance of 0.15 nm from the surface.

Regarding the 2A curve, the potential well is closer to the surface, in this case between 0.1 nm and 0.25 nm, establishing a more energetic bond with the adsorbent material.

Nonetheless, it is clear that the physisorption requires less energy to break the established bonds than the chemisorption.

This adsorption phenomenon can be used within diverse applications, such as vacuum technology, where the adsorption is used to achieve lower levels of pressure. For instance, by using a porous material we have a higher surface area to adsorb some undesired compounds that may be in the vacuum system. Furthermore, if we cool this material, we potentially increase its efficiency since it translates into a deeper energy well which consequently means it requires a higher energy to desorb the gas from that porous material.

An important information regarding the adsorption phenomenon and while working in this pressure levels is the time to adsorb a monoatomic layer. The equation that relates

the time formation of a monoatomic layer with the pressure, is given in equation 2.1:

$$\tau = \frac{n_m}{PN_A}\sqrt{2\pi MRT} \tag{2.1}$$

With τ the time formation of a monolayer in seconds, n_m the number of particles in a monolayer per cm^2, P the pressure in mbar, R the ideal gas constant, M the molar mass of the solid material and T the temperature in absolute units. A monoatomic layer will have approximately 10^{15} particles/cm^2 when fully covered [18].

For instance, it takes less than a second for a geometric surface area of 1 cm^2, under a pressure of $1{\times}10^{-5}$ mbar, to be covered with a monoatomic layer of air, assuming that the every particle that collides with the surface permanently adsorbs.

2.2 Thermal analysis techniques

There are several methods to do thermal analysis. Each of these methods focus on a different property, for example, thermogravimetry analyses mass, dielectric thermal analysis or the permittivity [20]. In this work, we pretend to analyse gases, specifically TCA that desorbs from cork substrates. Thus the thermal method that will be used is evolved gas analysis.

Evolved-gas analysis (EGA) consists on a technique that tracks the amount of gas or vapour that evolves from a sample, which is under decomposition or desorption, in function of time or temperature. The temperature of the sample has to be controlled [20].

A particular case of EGA is temperature-programmed desorption also called Thermal desorption spectroscopy (TDS), typically when experiments are performed using well-defined surfaces of single-crystalline samples under Ultra-high vacuum (UHV) system [19].

TPD experiments consist on letting gas or gases adsorb into a surface which will be posteriorly heated with a controlled (programmed) heating rate. The temperature increase is usually a linear function of time. While the sample is heated, gases desorb from the surface and are detected, by mass spectrometry.

The TPD techniques are relevant in the determination of kinetic and thermodynamic parameters of decomposition surface reactions or desorption processes [19].

It is possible to distinguish between different types of desorption. These are called orders of desorption and each order is separated regarding the process that originated it and the shape of the peak obtained, when analysing the adsorption. Figure 2.3 exhibits the different desorption spectra behaviours.

The desorptions of first order (2.3a) consists on an atomic or simple molecular desorption. It is independent of surface coverage and occur when a molecule adsorbs and then desorbs without dissociating. Its peak is asymmetrical with the higher temperature side having a faster change in the desorption rate.

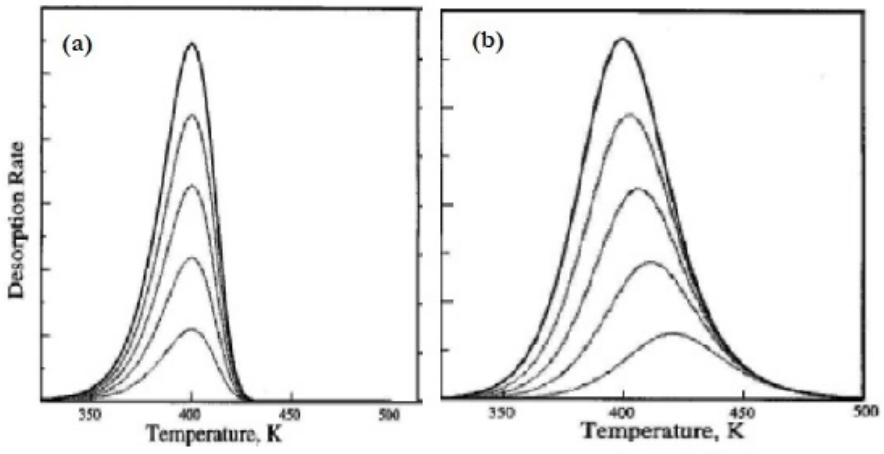

Figure 2.3: Different orders of desorption reactions. In figure (a) is represented the first order and in (b) the second order spectra. Figures adapted from [21].

The second order (2.3b) is a dissociative type of desorption. It is a result of when a molecule adsorbs and dissociates while doing it. The desorption peak of this spectra has a symmetric shape [21].

2.3 Adsorption analysis methods

In 1962, P. A. Redhead discussed methods of analysis regarding the thermal adsorption of gases. In it, the author described methods on how to determine the desorption energy, the rate constant of the desorption and the reaction's order from flash-filament desorption experiments [22].

Although the samples were heated by flash-filament method, which is a different process than ours, the adsorption parameters can still be obtained applying the methods described, as long as the temperature-time relation for the heating rate is properly controlled. Thus, methods for the determination of the desorption parameters previously indicated, will be described in this section and in chapter 5 will be applied to our data.

In Redhead's work, two different types of temperature variation were considered: a linear variation of sample temperature $T(t) = T_0 + \beta t$ and a reciprocal variation $\frac{1}{T} = \frac{1}{T_0} - \alpha t$. In both cases, t is the time variable, T_0 the initial desorption temperature and α, β the heating rates. In our case we will use a linear temperature variation with β being:

$$\beta = \frac{dT}{dt} \tag{2.2}$$

The desorption rate is often expressed by a rate law of n^{th} order [19]:

$$r_{des} = -\frac{d\sigma}{dt} = k_n \Delta\sigma^n \tag{2.3}$$

With σ being the surface coverage (molecules/cm^2), n the order of the desorption reaction and k_n the rate constant.

Notice that the reason for the existence of a desorption peak is due to the fact that TPD peaks are a convolution of surface coverage and rate of desorption. Taking into account that the surface coverage decreases with temperature, while the rate constant has a exponential factor that makes it increase with the temperature, it is expectable to find a desorption peak.

The rate constant indicates how fast the desorption process occurs. For example, while performing a TPD more molecules will desorb per unit of time as the temperature increases.

Knowing that the rate constant k_n is described by the *Arrhenius* equation we obtain:

$$k_n = \nu_n e^{-E/RT} \tag{2.4}$$

With E being the desorption energy of desorption and being expressed as J.mol, R the ideal gas constant in J.mol.K^{-1} and ν_n a pre-exponential factor, which in this case is related to the lattice oscillations or the frequency on which the adsorbed particles oscillate towards desorption, usually assuming a value of 10^{13} Hz.

Thus, the rate law is usually referred as the *Polanyi-Wigner* equation, defining the desorption energy E:

$$r_{des} = -\frac{d\sigma}{dt} = \nu_n e^{-E/RT_p}\sigma^n \tag{2.5}$$

If we now also consider the linear heating rate and substitute the time t in the *Polanyi-Wigner* equation 2.5 with $dt = (1/\beta)\, dT$ it yields [19]:

$$r_{des} = -\frac{d\sigma}{dT} = \frac{\nu_n}{\beta} e^{-E/RT_p}\sigma^n \tag{2.6}$$

Knowing that at $T = T_{max}$ the desorption rate has to be null and solving the differential equation:

$$\frac{E_{des}}{RT_p^2} = \frac{\nu}{\beta} n\sigma^{n-1} e^{(-E_{des}/RT_p)} \tag{2.7}$$

With this equation, Redhead determined that the temperature, T_p, at which the desorption peak's maximum is located is independent of the surface coverage while considering a first order desorption. Assuming a desorption of first order and then solving in order to the desorption energy E_{des}, we obtain the Redhead's general equation:

$$E_{des} = RT_p\left(ln\frac{\nu T_p}{\beta} - ln\frac{E_{des}}{RT_p}\right) \tag{2.8}$$

According to Redhead, the second parcel in the brackets is estimated to be 3.64. However, knowing a pair of T_p and E_{des} values, this estimated value can be confirmed. The

error introduced with this estimation is below 1.5%, when assuming a ν/β value between 10^8 K^{-1} to 10^{13} K^{-1} [22].

Obtained equation 2.8, it is now possible to determinate desorption energies for a single desorption spectra using a ν value of 10^{13}.

By plotting the desorption energy against peak's temperature we obtain the graph in figure 2.4:

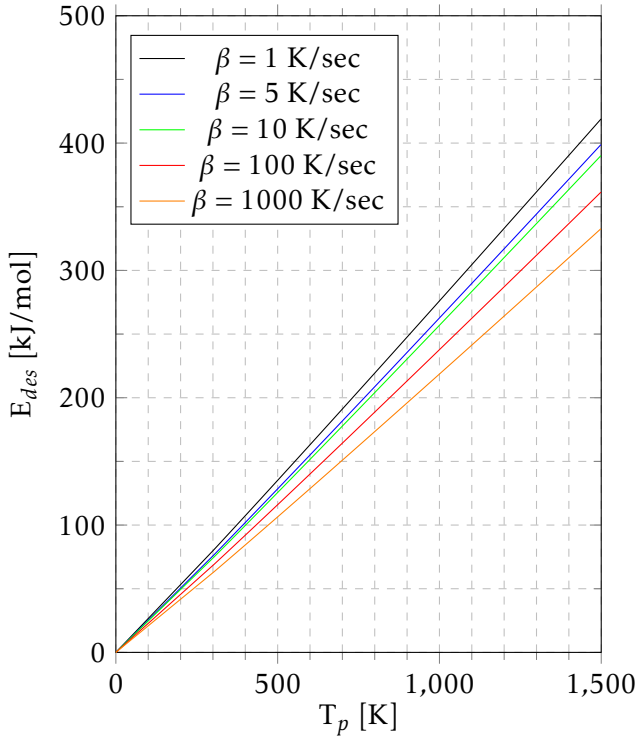

Figure 2.4: Relation between the desorption energy with peak's temperature for a first order desorption with a linear variation of temperature. Different heating rates were also considered.

It is possible to see the relation of E_{des} with the temperature of the maximum of the peak. Each curve represents a different heating rate which is defined by β, taking a pre-exponential factor of 10^{13} K^{-1}.

Considering both Redhead's general equation, equation 2.7, and the graph obtained in 2.4, it is possible to take conclusions. Regarding the temperature of the peak, if the heating rate is increased, we should expect to see the peak position shifting towards higher temperatures and having an increase in the desorption peak's intensity.

Still taking into account the relation between the desorption energy with temperature represented in the previous figures, we may still take some more conclusions towards the shift in the peak position. Thus, if we pretend to determine where the maximum peak's position of a certain desorption is found with a change in the heating rate, we may predict it with the curves represented in figure 2.4 or with Redhead's general equation, equation 2.7.

For instance, if we determine a peak's position, T_{p1}, as being 100ºC, while using a heating rate of 1 K/sec, we look at the 1 K/sec curve and determine the desorption energy. Then, using the curve corresponding to the heating rate that we pretend to use, we use the previously determined desorption energy to obtain the new peak's position T_{p2}. The desorption energy is characteristic of the system, meaning that it will not be changed with the heating rate and therefore we may use it to determine shifts in the position of peaks. Notice that the heating rate curves are represented in K/sec and not K/min, so that should be taken into account when predicting T_p values.

This method was the analysis described by Redhead to determine the desorption energy, however this may imply errors considering the assumptions that were done. Nonetheless it is a very useful method while obtaining an estimation for the desorption energy in desorptions of first order, since it is only required to determine the desorption peak's maximum experimentally, in order to obtain the desorption energy, which is the case of this work.

Alternatively, if we take equation 2.7 and apply the natural logarithm to both sides and rearranging, it yields:

$$ln\left(\frac{T_p^2}{\beta}\right) = \frac{E_{des}}{RT_p^2} + ln\left(\frac{Edes}{R\nu}\right) \tag{2.9}$$

Tracing the natural logarithm of T_p^2/β versus the reciprocal of temperature in absolute units, for a series of different β, we obtain a linear variation. Then, from the slope we determine the desorption energy and from the interception with the coordinates, the rate constant value. This alternative method is known as the heating rate variation method since for each curve different values of β are assumed.

Another method was proposed by Taylor-Weinberg-King as the complete analysis method [23]. This method allows a more precise determination of both E_{des} and the rate constant. It is applied in a similar way to the heat varying rate method. A natural logarithm is applied but in this case instead of using the general Redhead equation, we use equation 2.6, from which we obtain, after rearranging the equation 2.10:

$$ln(r_{des}) = ln\left(\frac{\nu_n \sigma^n}{\beta}\right) - \frac{E}{RT_p^2} \tag{2.10}$$

To further describe this method, we will be using an example in order to be easily understood. In figure 2.5 it is represented the complete analysis of a desorption spectra of silver from a rubidium substrate [21].

On the left side is represented a series of desorption spectra. In each there is a different initial surface coverage 2.5a. The first step is to integrate these spectra, obtaining the representation in 2.5b, and decide, based on the initial coverage, a coverage value from which a pair of coordinates (rate of desorption, temperature) will be determined - in this case a coverage value of 0.15 was chosen. Taking into account that this surface coverage value is reached at different temperatures, we may then obtain an Arrhenius-plot of the

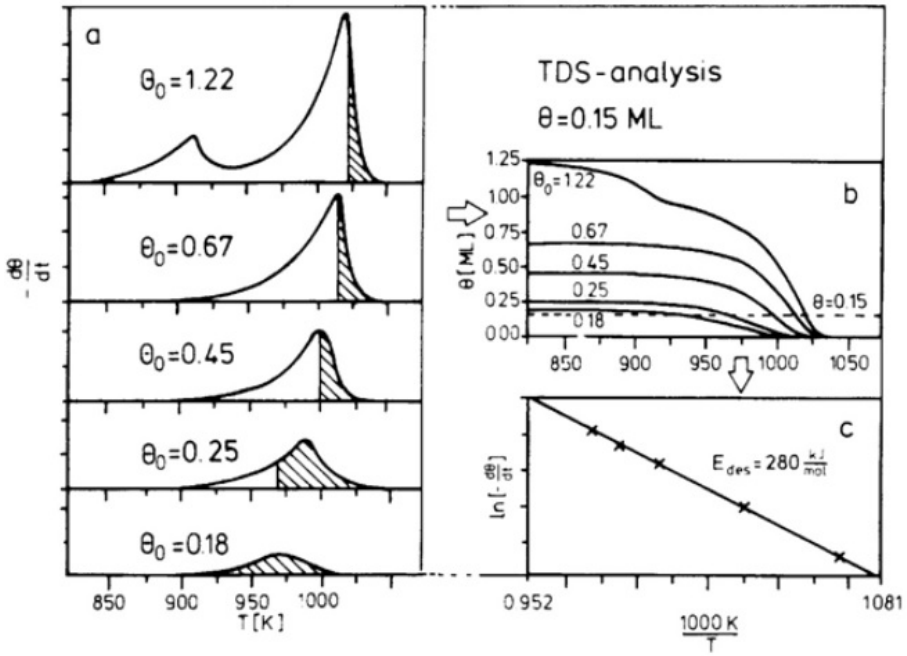

Figure 2.5: Diagram indicating the different steps of Taylor-Weinberg-King method for a desorption spectra of silver from a rubidium substrate. Image obtained from [21].

natural logarithm of the rate desorption $ln(r_{des})$ against the reciprocal of the temperature $1/T$, which is then represented in 2.5c. From it, it is possible to obtain the desorption energy by determining the slope.

2.4 Mass Spectrometry

To perform TPD, a technique to detect the desorbed species is required. Typically a mass spectrometer is used, as was our case.

A quadrupole mass spectrometer may be considered as having three main components: the ion source with the adequate optics of extraction, the analyser and the detector. The ions are produced typically by electron impact bombardment and the colliding electrons are originated by thermal emission from a heated filament [19]. In our case this filament was a tungsten wire and later it was replaced with iridium. Then, the ions that we pretend to analyse are guided by electrostatic lenses towards the analyser where they are selected taking into account their mass/charge ratios. The analyser consists of four parallel cylindrical rods and has applied voltages in order to filter the ions. If the ions travelling in between the rods are heavier or lighter than intended to, they are deflected from the path and do not reach the detector. The ions that reach the detector collide with collector and are then registered using a pre-amplifier. Besides the channeltron electron multiplier, there may be a pre-amplifier to further amplify the gain so it should be possible to do an easy analysis.

Notice that two spectrometers were used through the duration of this thesis work.

Even though they were the same model, the overall performance of the system increased after substituting the first spectrometer with the second equipment. The substitution took place before advancing towards the second phase of work and it improved a few aspects regarding the whole acquisition process. It allowed to perform faster data acquiring processes since it was possible to easily follow the peaks of interest with the mass spectrometer software. The observed intensities in each peak increased and instead of having large peaks covering more than two mass units, as it was observed with the initial spectrometer, the resolution improved and it was possible to see a peak in each mass unit. Since the detector allowed higher intensities to be observed, it was possible to afford a decrease of the adsorbate volume used in the contaminations, further described.

Both mass spectrometer, that were used in the experiments, have some parameters that have to be properly defined in order to achieve the calibration of the equipment and to allow the observation of the ions detected in the corresponding masses of the mass spectra. Otherwise, when performing TPD experiments the desorption spectra obtained could be misleading.

Thus the relevant parameters are mostly related with the extraction optics and the electrostatic lenses, which voltages are *extraction*, *deflection*, *focus*, *ion ref* and *QMA gnd*. For future reference, while using the same model equipment the values used are indicated in table 2.1.

Table 2.1: Parameters with the corresponding values after a calibration of the *balzers* equipment.

Parameter	**Value [V]**
Extraction	40.5
Deflection	258.6
Focus	26.1
Field Axis	9.8

Notice that while the *extraction*, *focus* and *field axis* parameters are measured regarding the *ion ref* parameter, the focus is measured in relation with the *QMA gnd*.

Another procedure worth noting about the mass spectrometer should be the special care about the mass spectrometer's filament, while introducing and changing samples. In order to preserve and keep the filament intact, the pressure should not be above 1×10^{-5} mbar, at least when the filament is working, otherwise the filament might get severely damaged and it is very likely that it might need a complete substitution.

Chapter 3

Cork and adsorbates

In the first part of this chapter, the cellular and the chemical constitution of cork are described. The cork cell's geometry is also discussed.

Later, in the second part of this chapter we focus on one of the main concerns of this work, the TCA as a cork contaminant. How it is formed and how it contaminates cork and consequentially wine, are subjects that will be approached. A detailed description on relevant properties of TCA is also done.

Ending this chapter, we discuss the reason for the selection of other substrates and adsorbates which were experimented in this work.

3.1 Cork - Origins and Constitution

Cork is the bark of the cork oak tree, *Quercus suber*, and is a raw material. It is characteristic tree of the Mediterranean region and it is obtained after the cork oak has attained a proper size to get its cork bark removed [24]. This procedure is done without damaging the tree. The cork will then regrow and within 8 to 10 years the process of removal is repeated.

This material has several applications, but the most acknowledged is as a stopper to wine bottles, preserving the beverage within.

It should be noticed that even though many other substitutes for cork were developed, these are only viable for the purpose they were initially developed [24], for example, synthetic bottle stoppers were designed solely for that purpose.

There is a huge preference for cork as far as bottle stoppers are concerned, and since it is a natural product, the wine producers seem to prefer having cork preserving their wine instead of any synthetic products. Nonetheless cork is a unique material with distinct properties and it is a material worth studying.

In the following sections, both the cellular structure and chemical structure of this material will be described.

3.1.1 Cellular structure

Robert Hooke (1635-1703) described cork using a microscope for the first time in the 16th century. He sketched and described this material as containing small holes which Hooke called cells from the Latin *cella* meaning small rooms [25]. Later, in 1950, Joaquim Vieira Natividade (1899-1968) observed cork using an optical microscope and gathered all information known about cork on a book of his own, entitled *Subericultura*.

Since Hooke's observation, it is known that cork is a cell material. These cells are structured like a honeycomb and shaped as prisms with their bases being typically hexagons. The cell walls are approximatelly 1.5 mm thick, being very thin compared to the rest of the structure. It is also possible to state that only 8% to 9% of the total volume is a solid fraction in early cork and 15% to 22% in late cork [25].

Different sections of cork's cellular structure are presented in the figure 3.1. Thus to have a proper understanding of the micrographs, three sections were assumed. The radial section is along the growing direction of cork and the tangential section is parallel to the vertical axis of the tree trunk. Both radial and transversal sections have the same axis, however, the transversal section is shifted by 90 degrees and it may be taken as a top or bottom view.

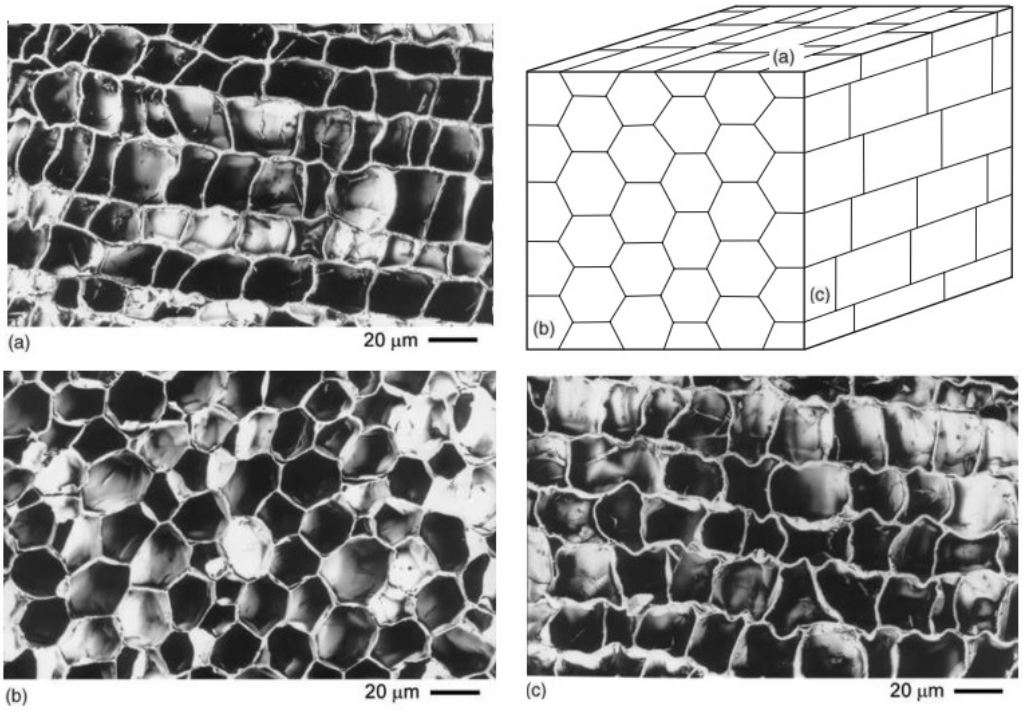

Figure 3.1: Cork's sections, with the respective scale, as observed with scanning electron microscopy: a) transversal; (b) radial and (c) radial section. A three-dimensional diagram of cork's structure is also presented adressing the respective sections. Adapted from [25].

Taking into account the micrographs presented, it is possible to evaluate the dimensions of the cork cells. The height of the prism ranges from 30 to 40 µm, the base edge from 13 µm to 15 µm and the cell's walls from 1 µm to 1.5 µm thick.

A relevant property is the cork density which has a mean value of 170 kg/m^3 and depends on the cells' density. It also depends on lenticular channels, on the cells' geometry and irregularities on the cell walls [26].

Another property to be considered while mentioning adsorption is the total internal surface of a cork's cell. Assuming an hexagonal prism with the already mentioned dimensions, we are able to determine the base area (4.4×10^{-6} cm^2 to 5.8×10^{-6} cm^2) and later the cell's total internal surface (3.2×10^{-5} cm^2 to 4.8×10^{-5} cm^2). Also knowing that the amount of cells ranges from 4×10^7 per cm^3 to 20×10^{7} per cm^3 (acknowledging both early cork and late cork), we may determine the total internal surface of an average sized cork (with a diameter of 2 cm and 4.5 cm high). Thus the number of cells in a cork bottle stopper are 5.7×10^8 to 2.8×10^9 and therefore we have an internal surface of 1.82×10^4 cm^2 to 1.35×10^5 cm^2 or 1.82 m^2 to 13.5 m^2. These results are gathered in the table 3.1.

Table 3.1: Relevant dimensions to obtain the total internal surface of an average cork stopper.

	Min Value	**Max Value**
Cell's Total Surface [cm²]	3.20×10^{-5}	4.80×10^{-5}
Number of Cells [cm⁻³]	4.00×10^{7}	2.00×10^{8}
Cells in a Stopper	5.65×10^{8}	2.83×10^{9}
Stopper's Total Internal Surface [m²]	1.82	13.50

3.1.2 Chemical structure

Cork is mainly constituted by suberin and lignin with suberin being the main component of cork's cell walls. Besides these components there are also polysaccharides and extractive materials.

The average chemical composition as it was determined by Pereira [26], is for suberin 39%, lignin 22%, polysaccharides 18%, extractive materials 15%, ashes 1% and carbohydrates which are mainly glucose and xylose. This study used virgin cork of 40 trees with no specific geographical location.

Suberin is a polymer made of long chain of aliphatic (non-aromatic) alcohols and acid monomers. While being more than a third of cork's material, it is the most abundant compound in cork and its percentage ranges from 33% to 50%.

The fact of suberin being hydrophobic contributes to the overall cork's impermeability. Besides that, suberin also contributes for the low conductivity and elasticity of cork [27].

It is a structural component of cork's cell walls which cannot be extracted without damaging the cork's cell walls and consequentially the cell's structure [25].

Lignin is the second most abundant of cork materials and is very likely to be decisive regarding the rigidness of cork's cell walls [26]. It constitutes in average 22% of cork's material and has variations which range from 20% to 25% within a single tree [26]. Lignin will be one of the substrates used in the experiments later described.

Polysaccharides are constituted by cellulose and hemicelluloses in similar proportions and correspond in average to 18% of cork's material [26].

Celluloses are linear polymers. In 1988, Pereira estimated that only 9% of cork's cell wall was cellulose, meaning that cellulose is not the most relevant component defining its chemistry or even its properties. Furthermore, the glucose associated to this material corresponds to approximately 50% of cork's monosaccharides [26].

Hemicelluloses are polysaccharides which are heteropolymers and are usually sorted by the main sugars present.

The extractive materials are waxes and non-polar compounds that are easily removed from cork using solvents such as water, alcohol or dicloromethane. The removal of such materials does not affect the cork's cellular structure.

Among the extractive materials it is possible to find all different types of molecules and chemical families. They are usually separated into the aliphatic group and the phenolics group, which are possible to extract using the mentioned polar solvents [25].

The aliphatic group consists of triterpenes (such as cerin, friedelin, betulin, betulinic acid and sterols), n-alkanes (from C16 to C34), n-alkanols (from C20 to C26) and fatty acids (such as monoacids, diacids and hydroxyacids) [25].

The phenolic group is composed of simple phenols (such as phenols, benzoic acids and cinnamic acids) and polymeric phenols (tannins) [25].

3.2 Trichloroanisole - Genesis and analysis

In the 80's, polychlorophenolic biocides such as pentachlorophenol, were used as fungicides, in order to protect some materials from microbes. However, there were some biocides that had 2,3,4,6-tetrachlorophenol (TCP) which was then metabolized by microbial action to 2,3,4,6-tetrachloroanisol - one of the compounds causing the cork taint in wines [28]. This compound was found to be carcinogenic and was prohibited. Later, it was substituted by 2,4,6-tribromophenol (TBP) but even though it did not cause any health issues, it would still be metabolised into 2,4,6-tribromoanisole (TBA) and end up having sensory attributes such as the mouldy and earthy odours that TCA also presents. TCP is also obtainable through the chlorine bleaching process of cork after the natural formation of phenol has occurred.

The common pathways for TCA formation are indicated in the figure 3.2. The molecule of TCA ($C_7H_5Cl_3O$) which has an average mass of approximately 211 mass units, is represented in red and it is possible to observe the disposition of the three chlorine atoms and the methoxyl radical (CH_3O).

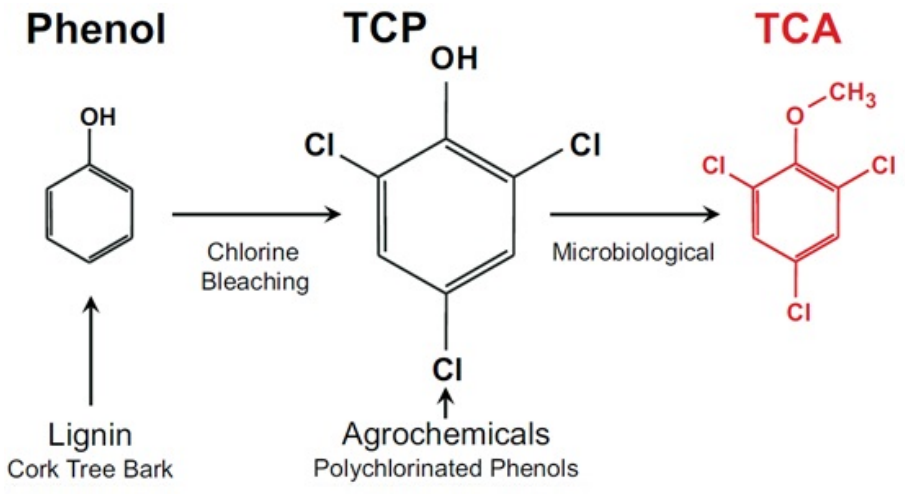

Figure 3.2: Diagram representing different paths of TCA formation [29].

Thus, TCA results of microbiological action in TCP, while TCP may originate either by naturally produced phenol which was submitted to chlorine bleaching from cleaning and hygiene products or simply caused by the application of agrochemichals. Re-used water in cork boiling processes may also contaminate subsequent cork pieces with TCA, even though it may be a superficial contamination [30].

We are interested in detecting TCA by mass spectrometry, thus we should know what to expect from its mass spectrum, which is presented in the figure 3.3.

Several peaks are presented in its spectrum so we focused on the most intense, since it would also be easier to detect. Therefore the peaks that will be followed are the ones at the masses 195, 197, 199 and 201. Besides the molecule of TCA, it is also represented in the mass spectrum of TCA the fragmentations that may occur within its molecule. Notice that the peak groups which have the same amount of chlorine atoms share the same shape.

It is possible to observe in the TCA spectrum, the fingerprint of the three chlorine atoms, not only in the peaks already mentioned but also in the peaks between masses 167 and 173 and between masses 210, and 216. This pattern is easy to identify based on the relative intensities of the individual peaks and on the group shape.

Chlorine has two stable isotopes which have masses of 35 and 37, with a relative abundance of 76% and 34%, respectively. Since the molecule of TCA has three chlorine atoms, there are four different combinations for these isotopes. These combinations translate into four peaks, each having a corresponding mass, regarding the chlorine isotopes that are present in TCA's molecule. Thus, the relative intensities of the peaks in relation to the most intense, are approximately, 95%, 30% and 3%, as it is possible to see in figure 3.3.

The phase diagram of TCA is also relevant in this work since we want to desorb TCA from cork substrates. In figure 3.4 are represented the phases of TCA and on which pressure-temperature region they are comprised. By crossing the blue frontier from the

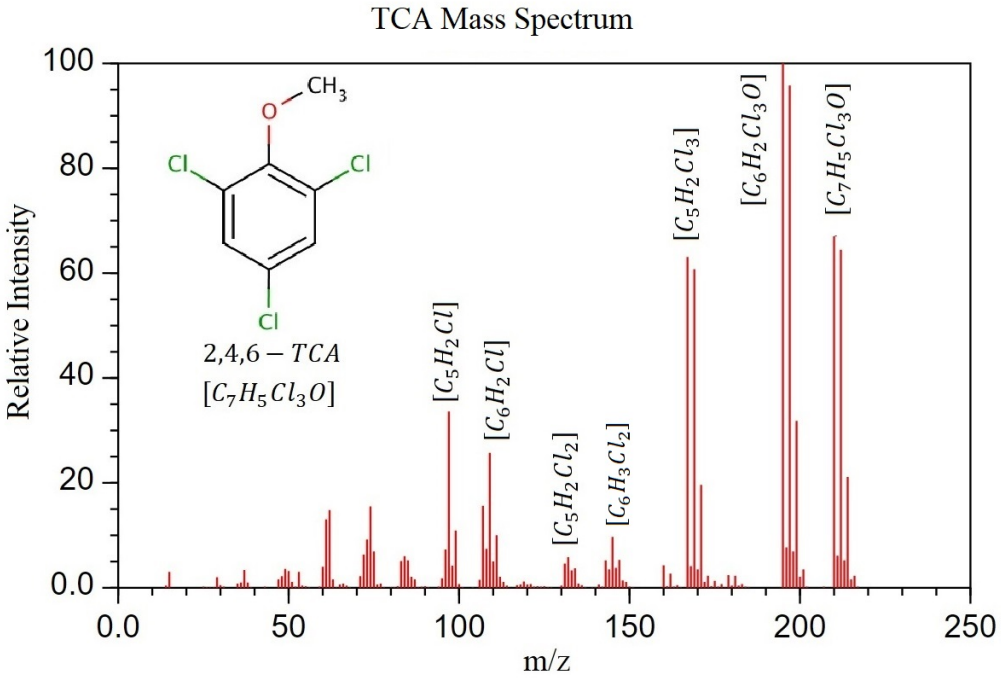

Figure 3.3: Mass spectrum of 2,4,6-trichloroanisole with its molecule representation. The expected molecule fragments are also represented in the respective masses. Adapted from NIST chemistry WebBook [31].

solid phase towards the gas phase, the sublimation of TCA occurs, by crossing the red frontier, TCA evaporates. The molar enthalpy of phase transition is 83.551 kJ/mol, from liquid to solid phase and of 61,969 kJ/mol, from gas to liquid phase (these enthalpy values are courtesy of an unpublished work of *Cork Supply*). The experimental melting point is at approximately 60°C (blue line).

Consider the triple point of TCA, which occurs at 58.9°C at a pressure of 0.823 mbar. Within these conditions, it is possible to find TCA in its three phases simultaneously. Above this pressure, TCA is also found in all phases, but it has to meet the proper conditions. For instance, consider a pressure a thousand times below the atmospheric pressure, of 100 Pa or 1 mbar. When the temperature is below 58.9°C, TCA is in solid phase, if it is above 62°C, it is in a gas phase. Below the triple point pressure, it is only possible to find TCA in its solid or gaseous phase.

There is TCA inside a flask at the secondary lines, which is in solid phase, and it has the purpose of being used as leak reference. Therefore, we intend that it stays in solid phase inside the flask. To prevent eventual losses by temperature changes, this flask is kept at room temperature inside a cup that is filled with water.

However, if we pretend to detect this TCA with the mass spectrometer, for eventual quantification purposes, we need to sublimate it. It should not be complicated to obtain the conditions to maintain TCA in vapour phase throughout the TPD experiments, since the main chamber of our vacuum system (further developed in chapter 4) is in high

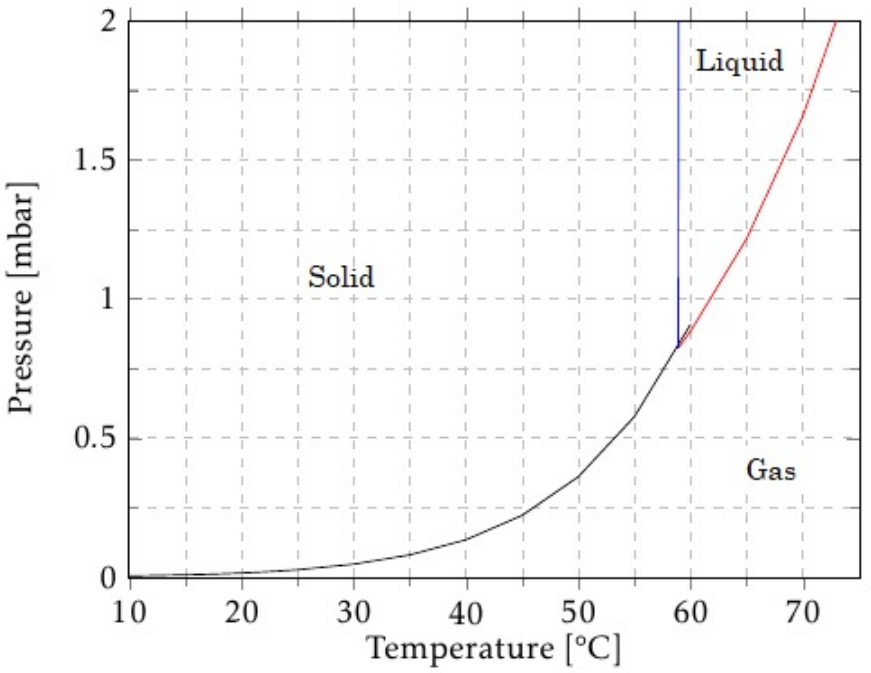

Figure 3.4: TCA phase diagram. Each coloured line is separating two different TCA phases. Blue line separates the solid from the liquid phase, red curve separates liquid from gas and the black curve is separating gas from solid phase. This diagram was courtesy of *Cork Supply*.

vacuum and the secondary lines are also connected to a rotary pump. Hence, as long as the pressure is below 2×10^{-2} mbar and the system is below a temperature of 23ºC, in both the main chamber or in the secondary lines, we guarantee that TCA is in vapour phase.

3.3 Substrates and adsorbates selection

In this work, different substrates and adsorbates were used. A simple piece of sliced cork will work as substrate, however two more types of substrates were used, lignin and cellulose. Unfortunately it was not possible to obtain suberin, the main constituent of cork, leaving this interesting variable to be tested in future experiments. The substrates were prepared, manipulated and sent to us by *RAIZ*, a laboratory from a well known paper producer.

Regarding the adsorbates selection, the decision was made taking into account the similarities of the compounds' chemical structure with the chemical structure of TCA (see figure 3.5a). Reminding the purpose of this thesis work, the intended goal is to study how TCA adsorbs into cork substrates, specifically how and which TCA's molecule group bonds with cork. For this purpose, we consider the different groups that compose its molecule - the three chlorine atoms, the methoxyl radical and the benzene ring - to decide the adequate compounds to be used as adsorbates. Thus, the compounds chosen

for adsobates were 1,3,5-trichlorobenzene (TCB) and anisole.

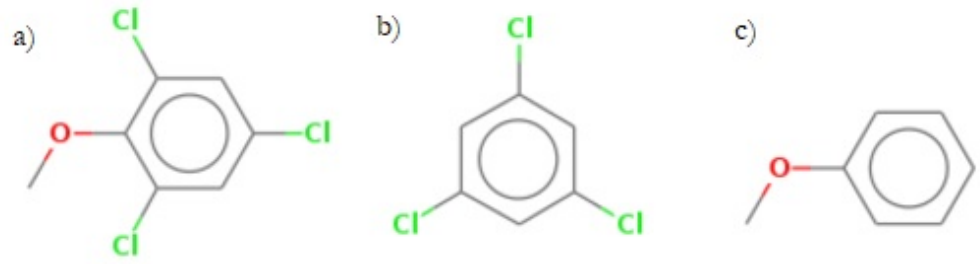

Figure 3.5: Chemical structures of the different adsorbates used: a) Trichloroanisole (TCA); b) Trichlorobenzene (TCB); c) Anisole. Adapted from NIST chemistry WebBook [31–33].

TCA is constituted by three chlorine atoms and a methoxyl radical which consists of CH_3O. Taking its chemical structure into consideration, two obvious choices come up: trichlorobenzene and anisole. While both share the same benzene ring, TCB was chosen due to the three chlorine atoms (figure 3.5b) that are present in the molecule of TCA and anisole was chosen since it shares the methoxyl radical with TCA (figure 3.5c). In other words, this decision was to determine whether it was the three chlorine atoms anchoring to the cork substrate or if it was the methoxyl radical.

The mass spectrometer had to be adjusted in order to detect the intended ion masses, whether it was detecting TCB or anisole. We have taken into consideration the mass spectra published at NIST's web page for both contaminants and for each we picked the most intense ones.

Regarding the mass spectra of trichlorobenzene (figure 3.6), the main peaks are at masses 180, 182 and 184.

For the anisole mass spectrum (figure 3.7), we followed the peak at 108 mass units and we often followed the peak at mass 78, in order to guarantee the mass calibration of the system.

Future experiments should explore contaminants such as chlorobenzene and tetrachlorobenzene to understand how are the chlorine atoms contributing to the TCA adsorption.

Having discussed the cork's constitution and the formation pathways for the TCA compound, it is now clearer the reasons for the selection of each substrate and adsorbate. With these notions gathered, it is possible to set the experimental conditions.

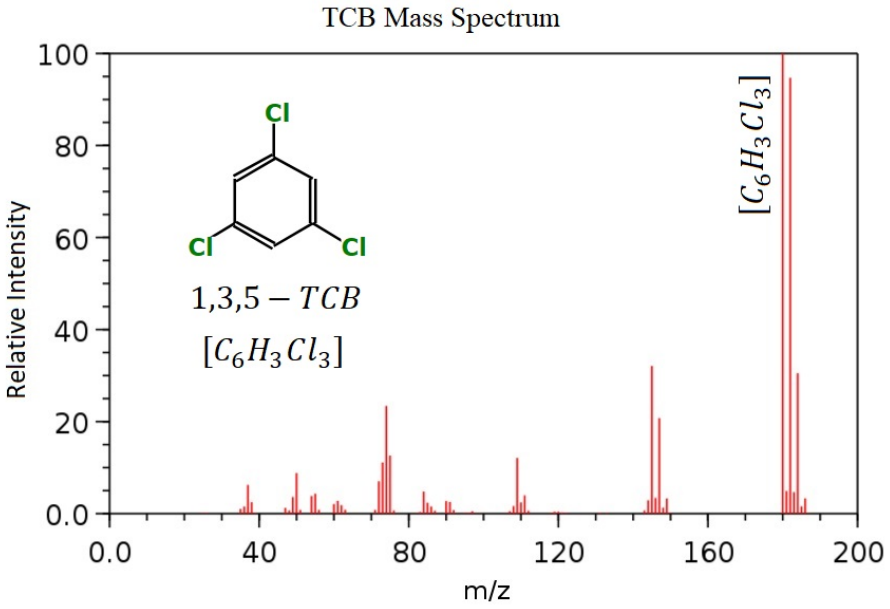

Figure 3.6: Mass spectrum of TCB. Adapted from NIST chemistry WebBook [32].

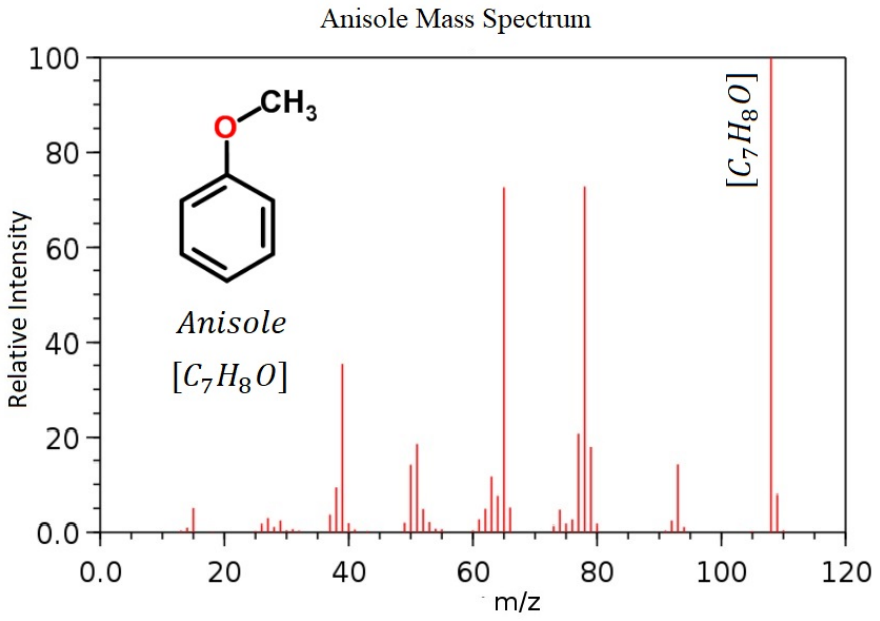

Figure 3.7: Mass spectrum of anisole. Adapted from NIST chemistry WebBook [33].

Chapter 4

Experimental Procedure

A detailed description of the vacuum system is done in this chapter, referring to which valves, pumps, different types of pressure gauges and different auxiliary equipment were used. Substrates preparation and contamination procedures are also described, for instance how the solutions were prepared and what was done in order to allow an easy reproduction of this process. A brief review on what we took into consideration while selecting the adequate heating rate is done in the final sections.

4.1 Experimental Setup

There were different set-ups, each one contributed to the improvement of the overall performance, however we will only focus and describe its last version.

4.1.1 Vacuum System

The vacuum system (see figure 4.1) is composed by two main pumps (a rotary P_1 and a turbomolecular P_2) connected to the main chamber and one auxiliary pump (rotary) which is pumping the other system segments. However, for better readability, two auxiliary pumps, P_3 and P_4, are represented instead of one.

The system can be divided in three sections:

- High vacuum system
- TPD sample holder
- TCA quantification

The first two sections are used in every test while the TCA quantification section is only used when testing a sample contaminated with TCA (later explained in this chapter).

Notice that if the vacuum system walls are at room temperature, it is easier for TCA molecules to adsorb onto them (see figure 3.4). Therefore, all sections were kept warm by heating tapes through the whole process, which were adjusted by a *Variac* autotransformer. Furthermore, the chamber was covered with aluminium foil to prevent heat losses as much as possible. This way, the main chamber was kept approximately at 100°C and the different segments were kept at approximately 75°C.

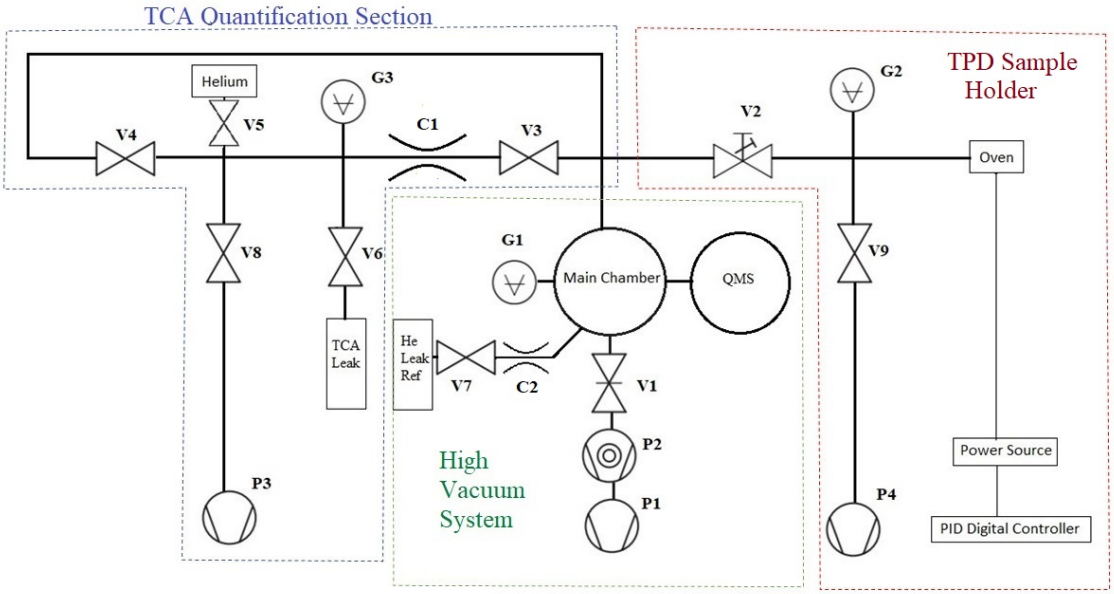

Figure 4.1: Schematic of the final setup of the vacuum system used.

The main chamber is a spherical chamber of 15 cm radius connected to the primary pumping system through a gate valve V_1, to the quadrupole mass spectrometer through a flange and to an helium reference leak also through a flange. This helium reference is relevant in the quantification method of TCA, further described in section 5.1. The chamber is also connected to the other two sections through a metering valve V_2 to the TPD sample holder section and through two different tube segments to the TCA quantification side. One segment has a needle valve V_3 and a flow restriction while the other segment has an in-line valve V_4. Besides that, the chamber also has a penning ionization gauge G_1 to measure the pressure in it.

It is in the high vacuum system section that it is detected and analysed the desorbed TCA coming from the contaminated substrates or from the TCA leak flask. The base pressure in it should be as low as possible in order to increase the free mean path of the molecules of interest, which consequentially translates into an increase of intensities measured, since less particle collisions will take place.

The pressure in the chamber ranged from 1×10^{-7} mbar to 1×10^{-5} mbar. This was observed even while continuously heating the chamber with the heating tapes and simultaneously heating the contaminated substrates in the TPD sample holder. There were only a few experiments that reached pressures out of this range.

In the TPD sample holder section there are a pirani gauge G_2 and an aluminium oven where the contaminated substrates stay through the TPD process. The reason for it to be aluminium is due to the high thermal conductivity of this material. The oven is surrounded by a resistance which is then connected to a power source, allowing it to heat to the desired temperature. The power source is an *Isotech 606D*, with enough power to keep the heating rate constant, even near the target temperature. For instance, a voltage of 24 V and 4.5 A were enough to reach 220°C, while keeping approximately the same heating rate.

The power source is then controlled by a Proportional-integrative-derivative (PID) controller. This equipment, which is an *Omron E5CC* digital controller, plays an important role in the TPD process. Given a heating rate, it allows, using its own algorithm and a solid state relay, to turn the power source on and off at its own pace, maintaining the desired rate. It is possible to adjust the PID constants, in order to avoid overshooting the target temperature and to reduce, as much as possible, the temperature oscillations at the target temperature.

Besides this controller, the oven also has a net inside itself as an accessory in order to compress the samples against the oven walls, so it guarantees that the samples are as close to the oven temperature as possible (see figure 4.2).

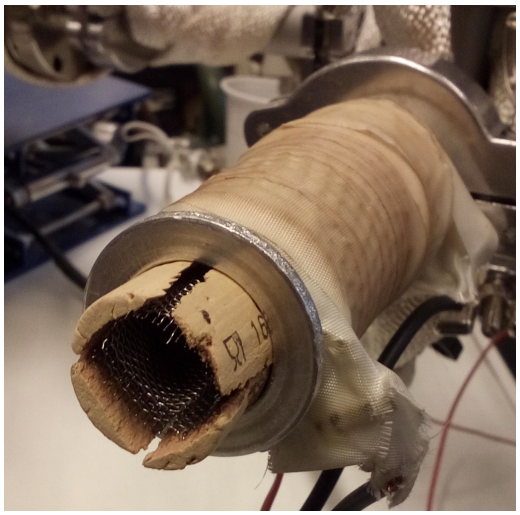

Figure 4.2: Picture of the oven with the auxiliary net compressing the samples against the oven walls.

The TPD sample holder section is connected to an auxiliary rotary pump P_4 through a copper pipe and to the TCA quantitative control through an in-line valve V_2.

The TCA quantification section has a pirani gauge G_3, an entrance that is often used with helium and a flow restriction C_1. This restriction is relevant while determining conductances, in the quantification method of TCA that it is proposed in this thesis. In this section there is also a flask containing TCA in solid phase, which is used as a reference while quantifying the detected TCA.

This quantification is important to determine if a desorption process is effective or not. By measuring the detected TCA, while performing a TPD, and knowing the amount of adsorbate used in the contamination, we have an idea of the desorption efficiency. The ideal case for a desorption process would be detecting as much TCA as the amount used in the contamination process.

There is always a chance that the TCA detected is desorbing from other material than the substrate. However, since the TCA readsorption cases were covered, whether by heating the chamber and tube walls or by the high pumping speeds, the amount of TCA detected due to this phenomenon should be negligible. Thus, we will be considering that the detected TCA is desorbing from the contaminated substrates.

Regarding the TCA's desorption origin in the substrate, it is difficult to precise whether the TCA is desorbing from the surface or from the substrate's bulk.

In a future work it is possible to improve the TCA's quantification section by building and installing reference leaks for the different adsorbates used and not just for TCA.

4.2 Samples Preparation

Different types of samples were used while trying to learn the physics of the desorption of TCA from a cork substrate. Four different types of substrates were used in this work, however the substrates that required more effort preparing were the cork substrates.

4.2.1 Substrates

Adsorption is a surface phenomenon. Therefore, an ideal substrate to test the TCA desorption would be an atomically flat layer of cork.

We are interested on studying the TCA that desorbs from the surface of cork. Hence, a first approach on a cork substrate consisted of eight slices of cork. These slices were sawed from the edges of two cork stoppers and were approximately 5 mm thick (see fig. 4.3). Each slice had an exposed area of 9 cm^2.

On later tests, the thickness of these slices was reduced to a thickness of about 1 mm, in order to decrease bulk contributions. To obtain this thickness a recently boiled piece of cork had to be sliced, otherwise the cork would break while slicing it.

Most of the substrates produced were used in TPD tests once, only a few exceptions were used more than once, but no noticeable change was observed in the obtained spectra.

4.2.2 Contamination Procedures

Substrates used were contaminated with the selected adsobates prior to the TPD experiments. This contamination process had to be consistent and reproducible, otherwise we would be introducing non intended variables to our process.

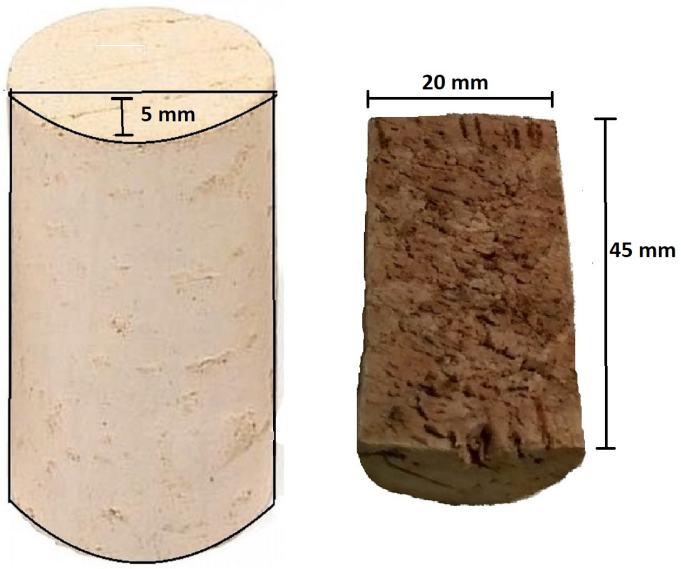

Figure 4.3: Representation of how the stoppers were cut in order to prepare the cork substrates and its approximate dimensions.

A mother solution for each of the contaminants was prepared. While TCA and TCB are solid compounds, anisole is in a liquid state, meaning that while preparing its solution there will be slight differences.

The solutions of TCA or TCB had a concentration of 1 g/L and the anisole solution a concentration of 1 cm^3/L. All solutions are contained on 100 ml Erlenmeyer flasks.

In order to obtain the concentrations for the solid contaminants, we weighted 0.1 g on a balance and added it to 100 ml of analytical ethanol, which corresponds to 79 g when weighted, since ethanol has a density of 0.79 g/mL. Then we dissolved the solute and it was assumed that the dissolution had a negligible increase on the final volume.

The main difference while preparing the solution for anisole consists on taking into account the volume of the liquid contaminant. Instead of weighting 79 g of ethanol, we measured 78.9 g, meaning that we added 0.1 ml of anisole to perform a total volume of 100 ml. In this case, we did not neglect the volume of the solute.

The contamination process was kept consistent. Using a syringe of 50 µl the contaminant was dosed and dropped on the surface of the subtrate. Notice that it was not injected. Initially a volume of 400 µl was used in the contamination process, however, after the replacement of the mass spectrometer the substrates required less amount of adsorbate to be properly detected, which lead to a decrease in the volume to 100 µl. Also notice that we used amounts of contaminant well above the detection threshold, to allow an easier detection, better define the shape of the desorption peaks observed and to study the different relations of the adsorbates with the different substrates.

After contaminating the substrates, the syringe had to be cleaned. To achieve a proper cleaning, the syringe was submitted to ultrasounds for 3 minutes, while filled with isopropanol. Besides the syringe, the oven and the net which was initially pulling the

samples against the walls of the oven also had to be clean with isopropanol.

4.2.3 Spray contaminations

A different type of contamination was tested in a final phase of work. It consists of a contamination procedure that uses spray flasks to contaminate the substrates. Each flask had a different contaminant that was transferred from the previously prepared mother solution.

When using these flasks to spray our samples, we would weight them before and after the contamination to know how much amount we were using when contaminating the samples. Notice that while spraying the substrate we tried to cover its surface as equally as possible. We limited ourselves to the thin slices of cork, when testing this contamination procedure, which was another approach towards observing the desorbed material that comes from the surface of a cork substrate and not from the bulk.

The results of this contamination process were inconclusive, meaning that more testing is required or that there is still room for improvements in either the contamination procedure or on the spray mechanics.

4.3 Experimental conditions

Different types of heating rates were used to conduct TPD experiments. Regarding the heating rate variable β, we had to determine which rate would suit best our needs.

While testing different heating rates, a trade-off was taken into account. We would either do a faster TPD, meaning that the desorption peakp would get shifted towards higher temperatures, or a slower TPD, that has a longer duration and the peaks position are more reliable since it is easier to maintain a slower heating rate rate than a faster heating rate.

In order to preserve the vacuum equipment, the TPD experiments consisted of a temperature sweep that ranged from approximately 30°C to 210-220°C. By not reaching temperatures above the 220ºC while doing temperature ramps, it would sometimes not be possible to observe the whole desorption spectrum.

This interval was enough to cover the temperature at which the peaks' maximum position occurred in the desorption spectra, as it was experimentally observed. However, it is possible to determine the peaks position prior to the TPD.

To find the expected temperatures of desorption we may follow and manipulate a process that Redhead described [22] and that is described in section 2.3. For instance, comparing an heating rate of 1ºC/min with a heating rate of 10ºC/min, a peak that has its maximum at 160ºC would be shifted by about 18ºC towards higher temperatures, having its maximum at 188ºC.

After a few experiments we decided to use a heating rate of approximately 5ºC/min, which allowed us to perform a TPD in 40 minutes.

Chapter 5

Results and Analysis

An extensive analysis and discussion of the experimental results is done in this chapter. We discuss how the quantification of the removed TCA is done and what are the desorbed species from a clean piece of cork. Later in the chapter, the desorption spectra related to each adsorbate and substrate used are analysed.

5.1 Quantification of the desorbed TCA

A method for the quantification of the desorbed TCA was proposed. This method was thought with the purpose of verifying the desorption process efficiency.

Reminding the experimental set-up described in chapter 4, a section was designed towards the quantification of TCA. In this section, a TCA reference leak and a flow restriction were introduced. This restriction guarantees a stable and known amount of gas into the mass spectrometer. There is also an entrance of gas, in this particular case, for helium.

In order to quantify TCA, a relation between our TCA reference leak and the released TCA from the substrates must be established. This relation is established by knowing the conductance through the flow restriction. Hence, by determining the conductance through the restriction for a known gas, for instance, for helium, it is possible to obtain the conductance for TCA.

The determination of the conductance for helium requires that the pressures in both sides of the restriction are known as well as the used gas flux of helium. For this purpose, a calibrated gas leak of helium was used. The leak, *VIC OM5-300*, had a leak value of 1.97×10^{-5} mbar.L/s, by the time of the experiments. A baratron pressure gauge was used to measure the helium pressure in the quantification gas line, during the conductance experiments. In equation 5.1 is represented the relation between these quantities.

$$Q_{He} = C_{He}(P_{He} - P_{Chamber}) \tag{5.1}$$

Which can be rearranged into:

$$C_{He} = \frac{Q_{He}}{(P_{He} - P_{Chamber})} \tag{5.2}$$

To determine the throughput of helium, Q_{He}, the signal measured in the mass spectrometer has to be taken into account. This signal is related to the partial pressure of helium, P_{He}, and to the pumping speed, glsS through a proportional constant, a, which encompasses, for example, ionization cross sections. (equation 5.3).

$$Signal_{He} = aP_{He}S \tag{5.3}$$

Knowing that the throughput of a gas is related to both the partial pressure and the pumping speed, we may rewrite the previous equation into equation 5.4:

$$Signal_{He} = aQ_{He} \tag{5.4}$$

Combining equation 5.2 and equation 5.4 it yields:

$$C_{He} = \frac{Signal_{He}}{a(P_{He} - P_{Chamber})} \tag{5.5}$$

Equation 5.5 still has into account the a constant from which we do not know the value. However, this constant has the same value for the helium reference leak, meaning that we may rewrite it as:

$$C_{He} = Q_{He,Ref}\frac{Signal_{He}}{Signal_{He,Ref}(P_{He} - P_{Chamber})} \tag{5.6}$$

Since it is possible to measure all quantities in this equation, an experiment was done to measure the conductance for helium. By controlling the pressure of helium, with a precision needle valve, in the quantification section, we did a series of measurements of the helium signal. After measuring the helium signal in the quantification section, we measured the calibrated reference leak in the main chamber. In order to measure each signal, we had to wait, typically less than a minute, to see the signal stabilizing and then measure it. Between each measure, we also made sure that the helium was pumped from the chamber and from the quantification section. This was confirmed by performing mass spectrometry in search of helium.

In figure 5.1 it is shown one of the results of this experiment. In this particular case, and in average values, the pressure in the quantification line was of 1×10^{-1} mbar, the pressure in the chamber of 3.26×10^{-7} mbar, and the respective signals $Signal_{He}$ of 3.35 and $Signal_{He,Ref}$ of 2.24. Considering that the calibrated helium leak, $Q_{He,Ref}$, has a value of 1.97×10^{-5} mbar.L/s, we obtain a conductance of 2.94×10^{-4} L/s for helium, through the restriction.

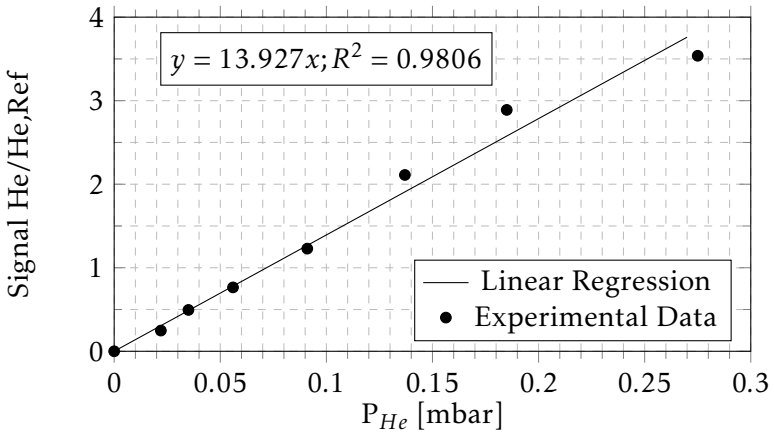

Figure 5.1: Relation of the calibrated helium signal with the helium partial pressure.

The typical values for the helium pressure in the quantification gas line and in the main chamber were between $1{\times}10^{-2}$ mbar and $1{\times}10^{-1}$ mbar and between $3{\times}10^{-7}$ and $7{\times}10^{-7}$, respectively.

This experiment was repeated three times. From these values we obtained an average conductance for helium of $2.47{\times}10^{-4}$ L/s.

Having determined, C_{He}, the conductance for helium, we were able to determine, C_{TCA}, the conductance for TCA through the restriction. The conductance is related to the molar mass of the gas, through an aperture, as represented in equation 5.7, with A being the section of the aperture:

$$C = A\sqrt{\frac{RT}{2\pi M}} \tag{5.7}$$

To apply this equation, the gas flow has to be under a molecular regime. This may be verified using the Knudsen's number (equation 5.8) which relates the free mean path, λ, with the diameter of the restriction, D.

$$Kn = \frac{\lambda}{D} \tag{5.8}$$

Being the free mean path expression represented in equation 5.9:

$$\lambda = \frac{k_B T}{\sqrt{2}\pi d^2 p} = \frac{7 \times 10^{-3}}{p} \tag{5.9}$$

In order to be in a molecular regime, the condition $Kn > 1$ has to be fulfilled. However, we do not know the diameter of the restriction, since it is a crimped capillary. Therefore we had to see if the relation of the calibrated helium signal with the partial pressure of helium was linear. Otherwise, a quadratic relation would mean that the flow was not under a molecular regime. As it is possible to see in figure 5.1, the relation is linear and thus we are able to use equation 5.7.

Considering this equation and relating the conductances for both helium and TCA, and then rearranging it, we obtain equation 5.10:

$$C_{TCA} = C_{He}\sqrt{\frac{M_{He}}{M_{TCA}}} \tag{5.10}$$

Knowing that M_{He} is 4 g/mol, M_{TCA} is 211 g/mol and that the average conductance for helium measured is 2.47×10^{-4} L/s, we obtain a conductance for TCA of 3.40×10^{-5} L/s.

With the determination of the conductance for TCA through the restriction, it is possible to determine the throughput of TCA that desorbs from the substrates. Applying the relations found in equation 5.1 and equation 5.4, that were used to determine the conductance for helium, we obtain equation 5.11 for the throughput of TCA:

$$Q_{TCA,Ref} = C_{TCA}(P_{TCA} - P_{Chamber}) \tag{5.11}$$

and for the signal of TCA, equation 5.12:

$$Signal_{TCA} = bQ_{TCA} \tag{5.12}$$

Then, combining these equations yields:

$$\frac{Signal_{TCA,Ref}}{b} = C_{TCA}(P_{TCA} - P_{Chamber}) \Leftrightarrow \tag{5.13}$$

$$\Leftrightarrow \frac{Signal_{TCA,Ref}}{\frac{Signal_{TCA}}{Q_{TCAunk}}} = C_{TCA}(P_{TCA} - P_{Chamber}) \Leftrightarrow \tag{5.14}$$

$$\Leftrightarrow Q_{TCAunk} = \frac{Signal_{TCAunk}}{Signal_{TCA,Ref}} C_{TCA}(P_{TCA} - P_{Chamber}) \tag{5.15}$$

By using the the TCA reference in the quantification gas line and knowing the pressure in both sides of the flow restriction, we may now determine the unknown flux of TCA, Q_{TCAunk}, coming from the contaminated substrates. Equation 5.15 may also be written as:

$$Q_{TCAunk} = \frac{Signal_{TCAunk}}{Signal_{TCA,Ref}} Q_{TCA,Ref} \tag{5.16}$$

Equation 5.16, $Q_{TCA,unk}$ can be expressed in the same units as $Q_{TCA,Ref}$, which could be for instance, µg/min, allowing a direct measurement of the desorbed TCA.

5.2 Desorption from clean cork

In this section, the desorption spectra of clean slices of cork are described. This experiment has the purpose of determining what are the desorbed species coming from a clean slice of cork. These desorbed species may contribute to the background of a TPD done with a contaminated substrate. The spectra were obtained with the mass spectrometer

Balzers QMS421 and processed with its own software, *Quadstar*. This software allows the possibility of having a three dimensional spectrum. However, that spectrum is plotted against the number of cycles instead of temperature, in which we were interested. Figure 5.2 is an example of this situation. In order to plot the spectra in function of temperature, a manual data treatment had to be done, since the software was not capable of doing such task. Besides that, the readability of the three dimensional spectra is reduced due to the perspective angles. For example, it is difficult to distinguish masses such as 17 or 18 in the 3D spectrum.

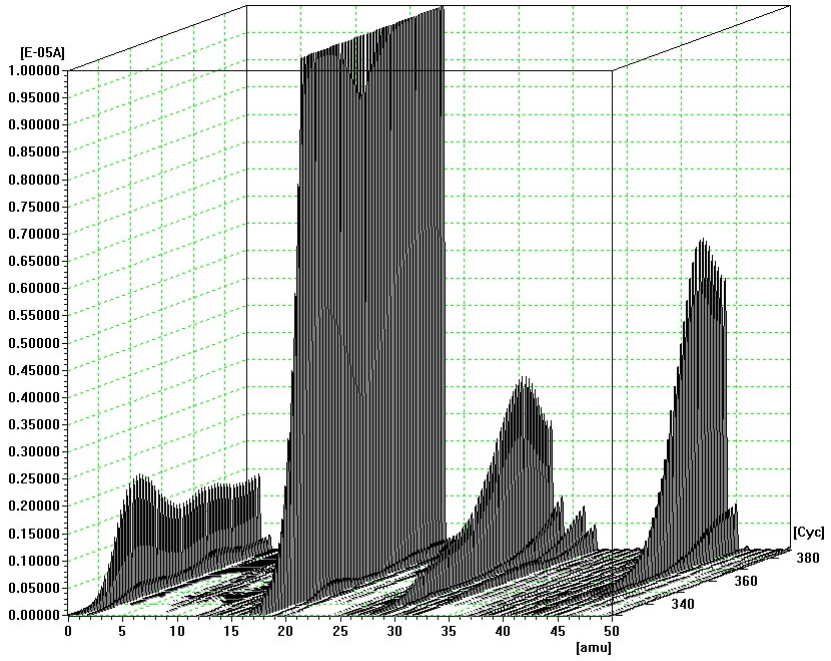

Figure 5.2: Example of a three-dimensional *Quadstar* software spectrum obtained.

The spectra which will be presented and discussed are of two dimensions but were extracted from the 3D spectrum, therefore its acquisition conditions have to be described.

The 3D spectrum consisted of cycles where a sweep of 200 mass units was done. The cycles were approximately 4 minutes long and the temperature ramp was in the range of 1°C/min, meaning that each sweep covered 4°C. The base pressure was of 1×10^{-6} mbar and the maximum pressure of work was of 2.5×10^{-5} mbar, at approximately 100ºC, which meant that the cork substrate still had a huge amount of water vapour adsorbed.

In figure 5.3 are represented the desorption spectra of two clean samples. These plots are semi-log on the y-axis in order to cover the different peak intensities measured. Each column represents a sample and each spectrum shows what are the desorbing species at different temperatures. The temperatures shown in the figure are, from top to bottom, approximately 30°C, 160°C and 220°C. The temperature sweep for the TPD is between 30°C and 220°C, which explains the reason for two of the temperatures. The 160°C is a relevant temperature that will be described further in this chapter. Notice that since these spectra

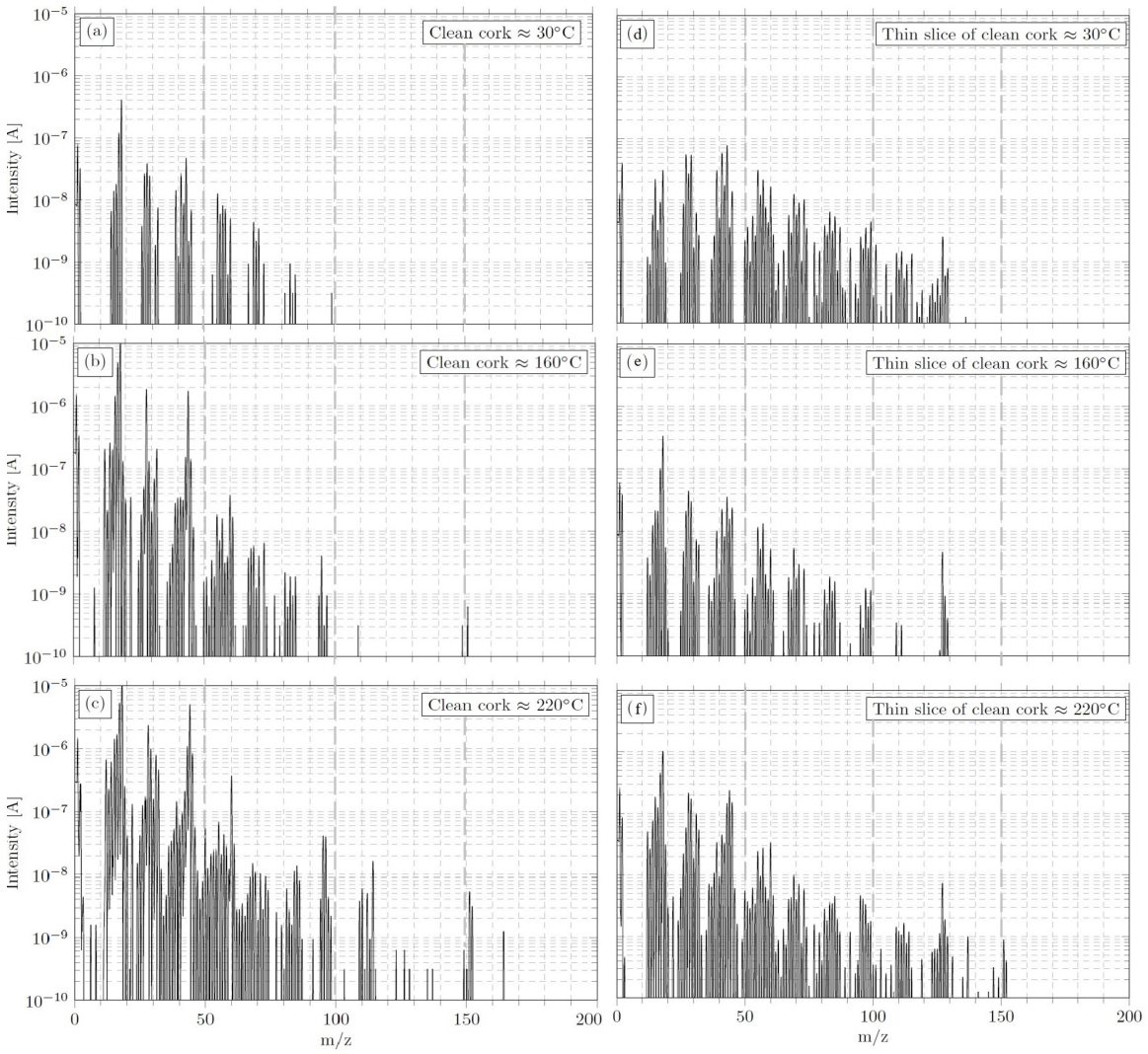

Figure 5.3: Desorption Spectra of clean slices of cork. In the left column the slice was approximately 5 mm thick and in the right column it was approximately 1 mm thick. Each row of spectra corresponds to a relevant temperature in the desorption of TCA.

were obtained from the 3D spectrum, which has cycles of 4 minutes, each desorption spectra represented in this figure covers 4°C. For instance, in figure 5.3a, the desorption started at 30°C but it ended close to 34°C.

In the beginning of the TPD at 30°C (figure 5.3a), a clear presence of water vapour is observed at mass 18. This peak is the most intense throughout the whole TPD experiment, as it is possible to observe in figure 5.3b and figure 5.3c. Besides the water vapour mass peak, other species peaks are expected within a high vacuum system. These species, that in this particular case are less intense, are the natural occurring diatomic molecules, H_2, O_2 or N_2 which are found in the first 50 mass units, respectively at masses 2, 16 and 28. Hydrocarbons, which are composed by carbon and hydrogen atoms, are also to be expected in this situation, with a lower intensity.

By increasing the temperature, other species begin to desorb from the cork substrate.

For instance, in figure 5.3b, at 160°C, a peak at mass 109, that was not present in the desorption spectra in the beginning of the TPD is observed.

In order to identify the hydrocarbon mass peaks that are present in the desorption spectra of the clean cork substrates (figure 5.3), the mass spectrum of a cork's extractive, which is an hydrocarbon, is considered. Fulfilling these conditions (see section 3.1.2) are hydrocarbons from C-16 (hexadecane) to C-34, (tetratriacontane). Since we are only analysing the first 200 mass units, the C-16 mass spectrum (figure 5.4), which has a molecular mass of 226.41 g/mol, is enough to cover this region and to see what are the hydrocarbon contributions.

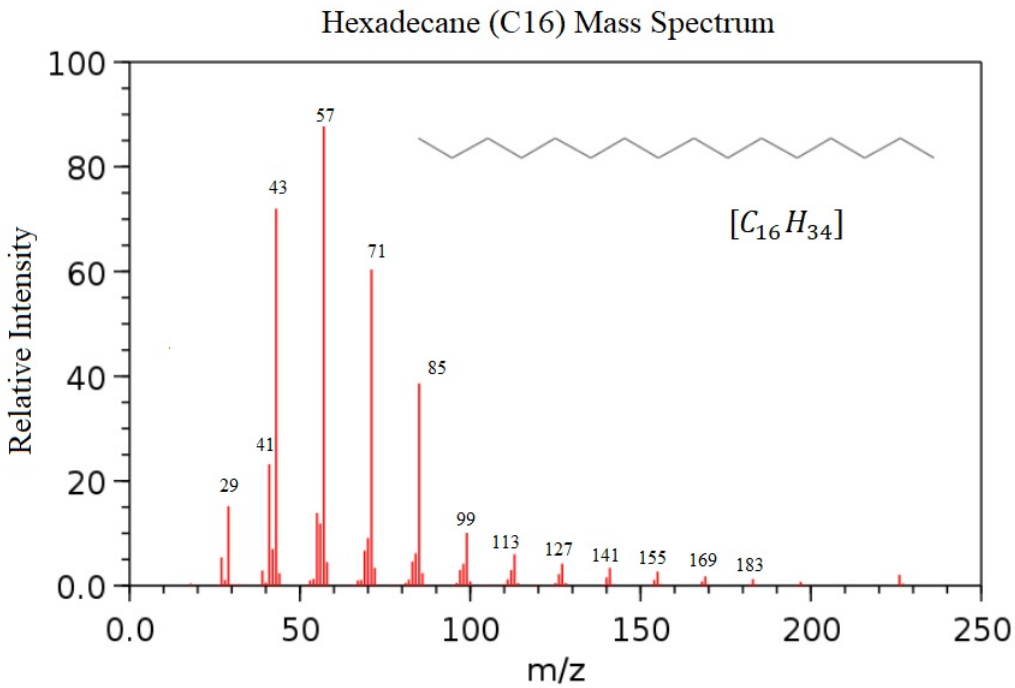

Figure 5.4: Mass spectrum of the hydrocarbon C16 (hexadecane) and its chemical structure. Adapted from NIST chemistry WebBook [34].

Thus, peaks at masses 41, 43, 57, 71, 85, 99, 113, 127, 141 and 155, match with the mass peaks observed in the desorption spectra of the clean slices of cork, specifically the ones that were obtained at approximately 220°C, where it is possible to observe all the hydrocarbon contributions.

This experiment was repeated with a thin slice of cork (approximately 1 mm thick) which is represented in the right column of figure 5.3. Besides the thickness difference, the remaining acquisition conditions were the same. The base pressure of work was of 1.6×10^{-6} mbar and the maximum pressure of work was of 1.1×10^{-5} mbar by the end of the TPD. Notice that unlike the first experiment, the maximum pressure did not occur at 100°C, which can be explained with the reduced thickness of the substrate. By having less cork cells, there was less water vapour adsorbed.

Despite the decrease in the thickness of the substrate, there is a prominent peak at

mass 127 in all desorption spectra of this substrate. In the first experiment the presence of this peak only seemed to appear by the end of the TPD. However, in this case, it was present since the beginning of the TPD. This mass peak still seems to correspond to a hydrocarbon as already mentioned for the first experiment.

By the end of the TPD at 220°C, it is possible to observe that the higher the mass, the less intense are the peaks. This similarity to the hexadecane's mass spectra seems to corroborate the idea that the peaks present in figure 5.3 at the masses indicated in figure 5.4 are hydrocarbons.

Another TPD experiment was done to the same thin slice where and was observed that the intensity of the peak decreased.

Considering that both substrates had the same experimental conditions, the reason for the lower intensities in the desorption spectra should be related with the thickness of the substrate. While the desorbed species of the thick slice saturated the detector at a given temperature, the desorbed species from the thin slice did not. A thickness decrease means less surface to adsorb, which consequently means lower intensities of the mass peaks.

Nonetheless, from mass 150 to mass 200 the contribution of the desorbing species are negligible. This is relevant since the TCA mass spectrum has its most intense peaks at 167, 195 and 210. Thus, when desorbing TCA from cork substrates, if there is a mass peak at these masses, they correspond to TCA and are not related with the cork extractives.

5.3 Temperature programmed desorption of TCA on cork

One of the first desorption spectra obtained combining TPD technique with QMS is represented in figure 5.5. The spectrum confirmed that TCA does in fact desorb, and that the temperature has a relevant role in its desorption.

The samples used to obtain this spectra consisted of eight slices of cork contaminated with the TCA solution previously prepared (see section 4.2.2). A total volume of 400 µl of TCA was equally divided by the slices. Knowing that the solution of TCA had a concentration of 1 g/L, a total mass of 400 µg of TCA was used in this experiment.

In order to dry the substrates and remove water from them, slices of cork were heated to 100ºC before the contamination process. After contaminating the substrates with TCA, they were heated again to a temperature of 50ºC. The reason was to simulate as much as possible the drying process of cork bottle stoppers that the cork sector typically does - the stoppers are usually left on a heated atmosphere to dry. This procedure contributes to a decrease of contaminated cork stoppers found on contaminated wines. The drying process, in our case, also contributed towards lowering the working pressure in the experimental set-up.

In this early phase of work, the data acquiring process was not optimized, therefore

the heating rates had to be lower than intended. Only after replacing the mass spectrometer for a better one it was possible to further increase the heating rate to 5°C/min. Thus, a heating rate in the range of 1°C/min was used, performing a total of three hours manually acquiring data for each desorption spectra. The temperature sweep was from 30°C to 210°C, the peak has a full width at half maximum (FWHM) of near 50ºC and the desorption rate reaches its maximum at 162ºC.

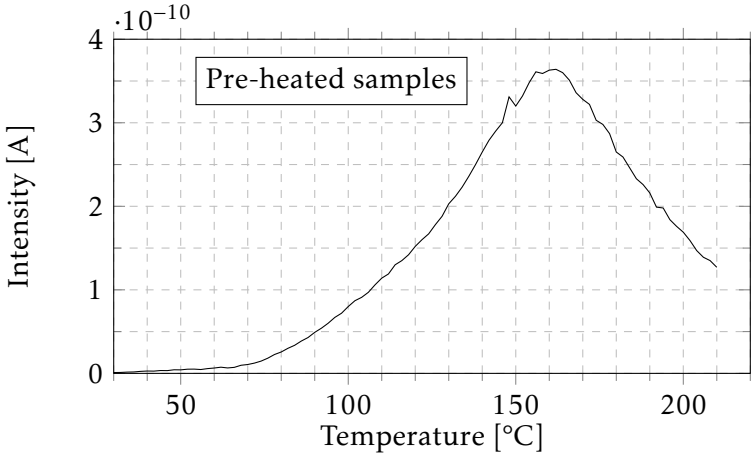

Figure 5.5: TCA desorption peak in a cork substrate.

It is difficult to precise the end of the desorption, but it is possible to estimate the TCA removed in this interval, using the TCA reference leak and the method described in section 5.1. Equation 5.17 is the expression used to determine the desorbed TCA detected during a TPD experiment:

$$Q_{TCAunk} = \frac{Signal_{TCAunk}}{Signal_{TCA,Ref}} C_{TCA}(P_{TCA} - P_{Chamber}) \tag{5.17}$$

In this particular case, the average pressure in the main chamber was of 4.41×10^{-7} mbar and in the TCA gas line was 3.69×10^{-2} mbar. The TCA signal can be seen in the figure 5.5 and the TCA signal of reference, which was measured after the TPD experiment, had a value of 5.74×10^{-10} A. Even though the TPD experiment had a duration of approximately three hours, the drift in the signal measured for the TCA reference, should be negligible. By the end of the TPD, a cumulative amount of 294.3 µg had been removed, which is 73.6% of the initial amount used to contaminate the substrate.

Regarding desorption energies, if we apply the Redhead's analysis method (see section 2.2) in this desorption spectra and in the following data that was obtained in this work, we may estimate the desorption energy for each found peak. Equation 5.18 reminds what has to be taken into consideration:

$$E_{des} = RT_p\left(ln\frac{\nu T_p}{\beta} - 3.64\right) \tag{5.18}$$

Knowing that the peak's maximum is at a temperature of 435 K, the ν is 10^{13} Hz and the β is $\frac{1}{60}$ K/sec, we estimate a desorption energy of 131.9 kJ/mol.

A second TPD was done with the same sample used to obtain the spectrum in figure 5.5 and without any further contamination. That experiment confirmed that the TCA was removed beyond the detection threshold of the equipment by heating to 210°C.

In figure 5.6 it is represented a desorption spectra of TCA from cork, which was done under the same experimental conditions than the previous experiment, with the only difference being that it was not pre-heated at 50°C. There is one peak at 158°C, very similar to the one previously observed, and another peak was detected, which in this case is more intense, has its maximum at 64ºC and has a FWHM of 50ºC as well. This peak, that requires less energy to be detected, could be TCA being desorbed from cork cells or a TCA sublimation.

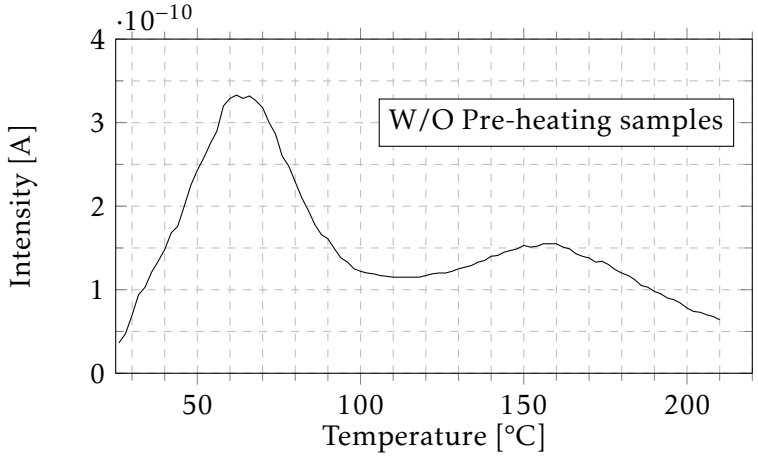

Figure 5.6: TCA desorption peak in a cork substrate without pre-heating at 50ºC after contamination.

Applying the same method as in figure 5.5, the estimated desorption energy for the less energetic peak is 101.5 kJ/mol and for the most energetic peak is 130.7 kj/mol.

Considering the TCA signal observed in this figure, the TCA reference signal of 8.84×10^{-10} A and an average partial pressure of TCA in the quantification gas line of 3.52×10−2 mbar, we determine that approximately 185 µg of TCA were detected after this TPD, which corresponds to approximately 49% of the initial TCA.

Nonetheless, it seems clear that the pre-heating process is relevant towards the removal of the lower temperature peak.

5.3.1 Pre-heating effects on TCA desorption from cork

After noticing the differences in the desorption spectra with and without pre-heating, another experiment was done in order to find whether this peak at low temperatures was a desorption peak or not. In this experiment, 10 sets of eight cork slices were used and each set was used for a single experiment.

In figure 5.7 is represented the results of this experiment. Each graph has two plotted spectra for two sets of samples, which were experimented in the same day. The only exception is figure 5.7e, in which the samples were experimented in two separate days.

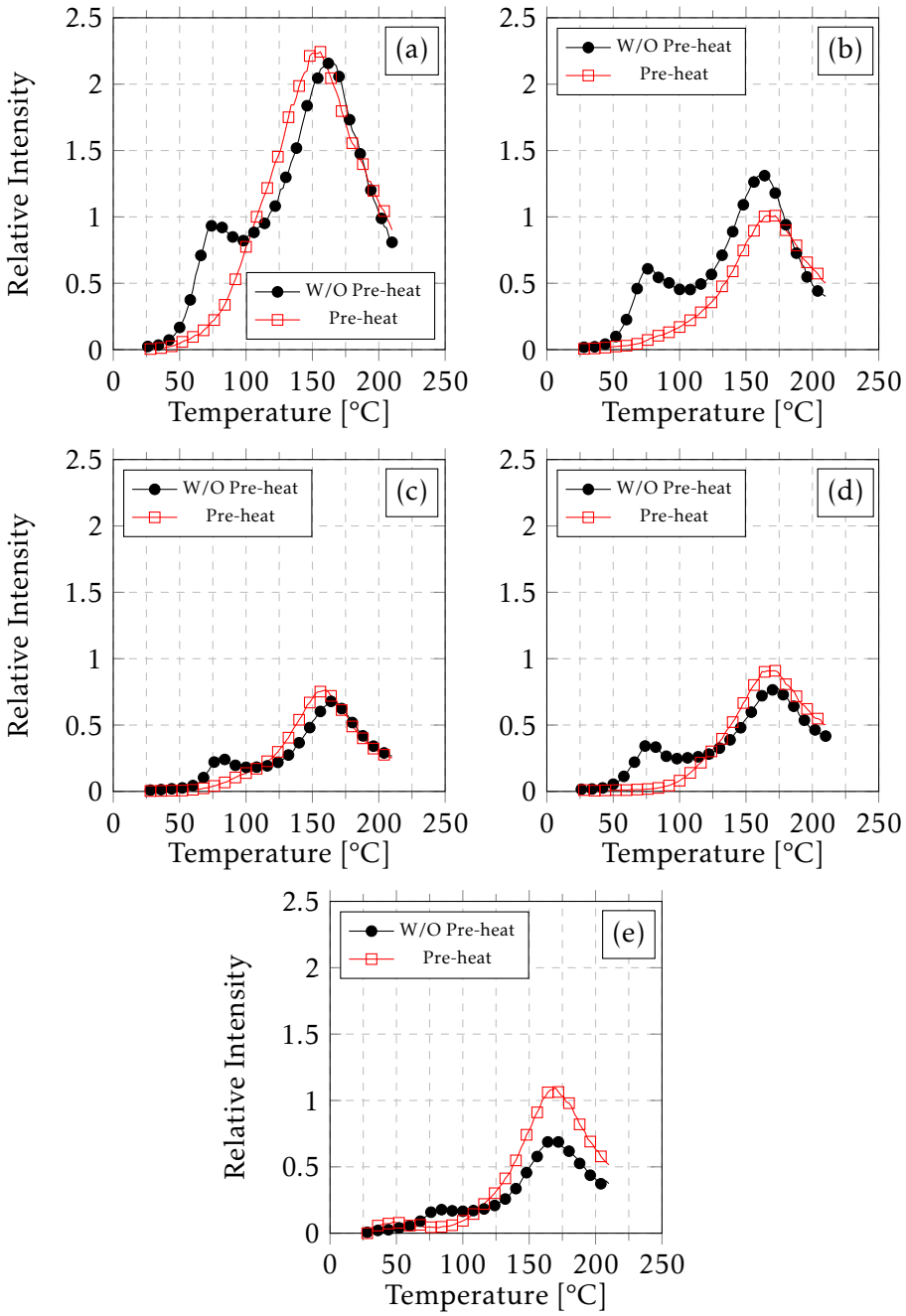

Figure 5.7: TCA desorption from cork substrates. In each graph, the circle marks represent the pre-heated samples and the square marks represent the samples that were not heated before the TPD process.

The experimental conditions consisted on a heating ramp of 1°C/min and a working pressure in the range of 1×10^{-5} mbar which typically had a peak at approximately 100°C that could be related with desorption of water vapour from the cork substrates. The

substrates were prepared as described in section 4 and contaminated with TCA, with a volume that corresponds to a mass of 400 μg. This volume was equally distributed in the surface of the eight slices of each set. Half of the contaminated substrates were pre-heated before the TPD experiment and the other half was not. The red squares represent the pre-heated samples and the black circles the ones that were not pre-heated after contamination.

After each TPD experiment, the TCA reference signal was measured so we could determine the TCA that was desorbed from the substrates by the end of it.

Analysing figure 5.7, each spectrum is calibrated in relation to the TCA reference signal that was measured in the TCA quantification gas line, after its TPD. Therefore the spectrum is has the y-axis in relative units which is plotted against temperature. Since all spectra are calibrated we can compare them.

In three of the five graphs, specifically in 5.7a, 5.7c and 5.7d, the proportions between the pre-heated curve and the curve of the samples that were not pre-heated seem to be constant. The shape and the maximum's position of both peaks are also similar and seen at the same temperature. Concerning these features, figures 5.7b and 5.7e are different. In figure 5.7e, these differences could be related to the fact that the experiment was done in different days, meaning different experimental conditions. In 5.7b, it could be explained with the voltage adjustment of the heating tape, which was unintentionally different between these two experiments.

The purpose of this experiment was to verify if the low temperature peak was due to TCA desorption or a change in phase. One approach should be using the quantitative method already described in section 5.1 and verify if the lower temperature peak is getting desorbed by comparing peak areas. On the one hand, if the area under the square marked curve was less than the area under the circle marked curve, that would mean that the less intense peak in the non-heated samples was getting removed from cork, which would consequently mean that it was a TCA change of phase and that it was easily removed by the pre-heating process. On the other hand, if both areas had the same value, that would mean that the lower temperature peak in the circle marked curve represented TCA desorbing from cork but then it was getting re-adsorbed back into the cork substrate establishing higher energy bonds.

Calculating the integrals for each pair of curves and comparing it, we noticed that the values were relatively close (with the exception of two graphs 5.7b and 5.7e) and so were the removed TCA percentages, which could mean that TCA was getting re-adsorbed. However, since none of the TCA desorption spectra was fully obtained, the quantitative method could not be used in this particular scenario as effectively as intended. A better determination of the integral value could be obtained if at least the higher temperature section of the spectra matched in both curves in each graph.

We may determine an average value for the desorption energies for both peaks observed in each curve. The peak's maximum position for the lower temperature peak was between 74ºC and 80ºC, while the higher temperature peak was between 156ºC

and 166ºC. The average desorption energy is 105.4 kJ/mol and 131.9 kJ/mol, respectively. For the desorption energies of each peak in each graph, see appendix A.1.

5.3.2 Sidetrack experiments

In this phase of work, different materials, such as aluminium, stainless steel and polytetrafluoroethylene (or, as it is commercially designated, teflon), were contaminated with TCA and experimented. This experiment was done in order to see if parts of the vacuum system could compromise the results.

In figure 5.8 is a desorption spectra of a piece of teflon that was contaminated with 400 μg of TCA. A desorption peak is found at a temperature of approximately 160°C. Notice that this desorption spectra intensity is two orders below the typical intensities observed, for example, in figure 5.5.

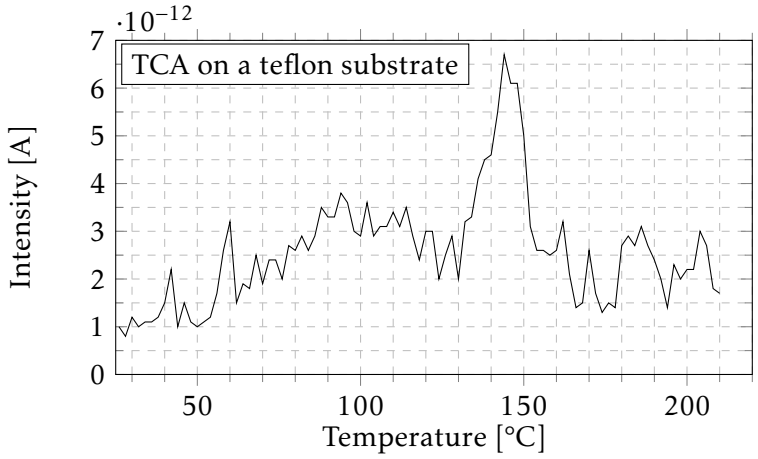

Figure 5.8: Desorption spectra of TCA on a teflon substrate.

Although it was possible to observe a TCA desorption peak on a teflon substrate, the TCA present in the rest of the materials did not have a clear TCA desorption peak. This means that the desorbed species coming from the experimental equipment are negligible, comparatively with the TCA desorbing from cork substrates or that TCA is not adsorbing onto the parts of the vacuum system at all.

This experiment was repeated and a similar peak was found at the same temperature of approximately 150°C. However, the hypothesis of the desorption peak being occasional should not be completely put aside within these orders of intensity.

Besides the material experiments, a particular experiment concerning the pumping procedure was done. It consisted on pumping eight slices of cork already contaminated with TCA for a week at a temperature of 25°C and in the pressure range of $1{\times}10^{-6}$ mbar. This had the purpose of determining how the pumping procedure affected the desorption spectra and to confirm that even after a whole week of pumping the contaminated substrates, the adsorbed TCA would still be detected with a temperature treatment.

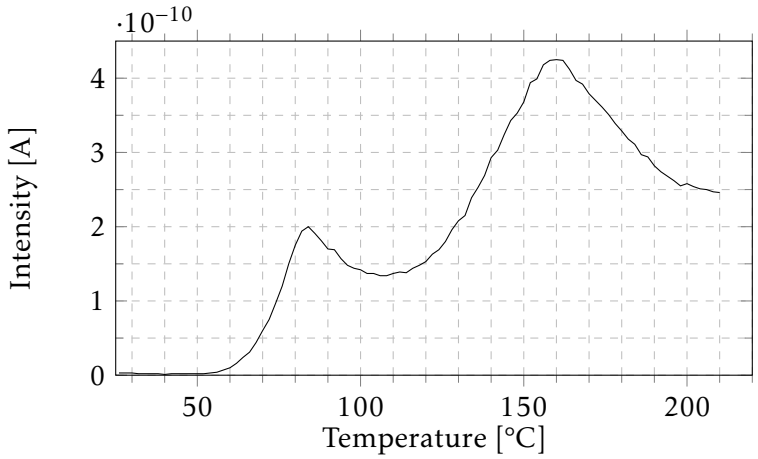

Figure 5.9: Desorption spectra of TCA on a cork substrate obtained after pumping the samples for a week, in a high vacuum system.

Observing figure 5.9, is possible to see that the most intense peak is the higher temperature peak, at 160°C, instead of being the lower temperature peak, at 84°C, as it happened in figure 5.6. Since the spectra has approximately the same shape observed in figure 5.6, it means that we are removing TCA that is adsorbed on cork with an increase of the temperature, and the pumping procedure is not sublimating any possible TCA crystals. If they were to be sublimated, the pumping effect at the referred pressure of about $1{\times}10^{-6}$ mbar should be enough to remove the TCA crystals.

5.4 Desorption from cork-related substrates

The intended goal for this thesis is to understand how the TCA molecule adsorbs and which group of it is effectively contributing towards the adsorption process in cork substrates. Hence, other adsorbates and substrates were chosen regarding the TCA chemical structure and the cork constitution, respectively.

In figure 5.10 are represented the desorption spectra of the adsorbates used to contaminate a cork substrate. The substrates used for this experiment consisted on four slices of cork, prepared with a total amount of 100 μg of TCA and a TPD heating rate of 5ºC/min. This increase in the heating rate and the decrease in the amount of TCA used was possible due to the replacement of the mass spectrometer, which also allowed an automatic data acquiring process with a duration of approximately 40 minutes. The substrates contaminated with TCA were not pre-heated to 50ºC before the TPD, as it was previously done and discussed.

In this figure, we verify the same shape of the TCA desorption spectra and that the peak at 86ºC is more intense than the peak at 161ºC. Even though the higher energy peak is not so clear in figure 5.10 and it only manifests as a shoulder peak, its maximum position is approximately close to the already mentioned maximum values in the previous spectra of TCA on cork substrates, for instance, in figure 5.6.

The shift towards higher temperatures in the maximum position of the peak can be explained with the increase in the heating rate, which was changed from 1°C/min to 5°C/min. In section 2.2 it was explained how to obtain, theoretically, the shift in the position of the peak, which in this case is of, at least, 10°C.

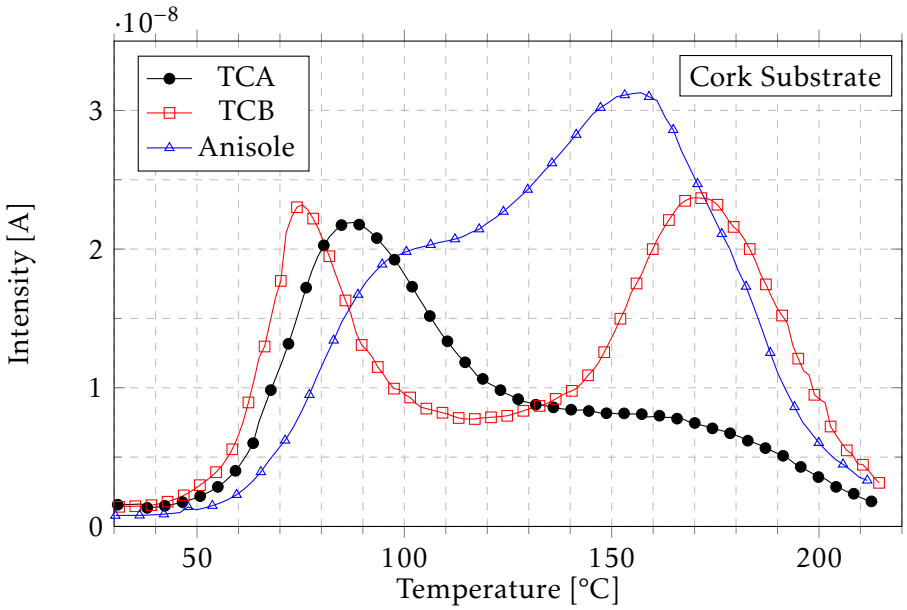

Figure 5.10: Desorption spectra of the different adsorbates while using slices of cork as substrate.

Figure 5.10 introduces the different chosen molecules as a variable in the desorption subject. The circle marked curve is the desorption spectra of trichlorobenzene, while the triangle marked is of anisole.

Regarding TCB, it is possible to observe two peaks. A low temperature peak at a temperature of 75ºC and a higher temperature peak at 170ºC. Both peaks have approximately the same intensity. TCB, having the lowest FWHM, has its peaks better defined comparing with the other two adsorbates. The lowest temperature peak has 30ºC of width at half maximum, while the highest temperature peak has 40ºC of width.

Anisole has two peaks, one at a temperature of 96°C and another at a temperature of 157°C. Its desorption peaks from cork are not as clear as with TCA or TCB. The lowest temperature peak, which is a shoulder peak, is not as prominent as the higher temperature peak and they are not completely resolved from each other.

Comparing with the desorption curve of TCA, the low temperature peak of TCB is slightly shifted towards lower temperatures and the low temperature peak anisole of anisole is shifted towards higher temperatures. The higher temperature peaks are less shifted in their position but either TCB or anisole still have a slight shift, even though it is less than 10ºC from the higher temperature TCA peak. Notice that the spectra were obtained with the same heating rate of 5ºC per minute, meaning that the shift should be equal to all desorption peaks.

All adsorbates seem to start desorbing from cork at the same temperature. Furthermore, the desorption temperature where it seems to end the desorption for each contaminant is practically the same.

The desorption energies of the lowest temperature peak and of the highest temperature peak are respectively 103.5 kJ/mol and 126.1 kJ/mol for TCA, 100.5 and 128.5 kJ/mol for TCB and 106.5 kJ/mol and 124.9 kJ/mol for anisole.

In figure 5.11, it is shown the desorption spectra of the different adsorbates from a different substrate, lignin. By changing the substrate to one of the main components of cork, clear differences are noticed.

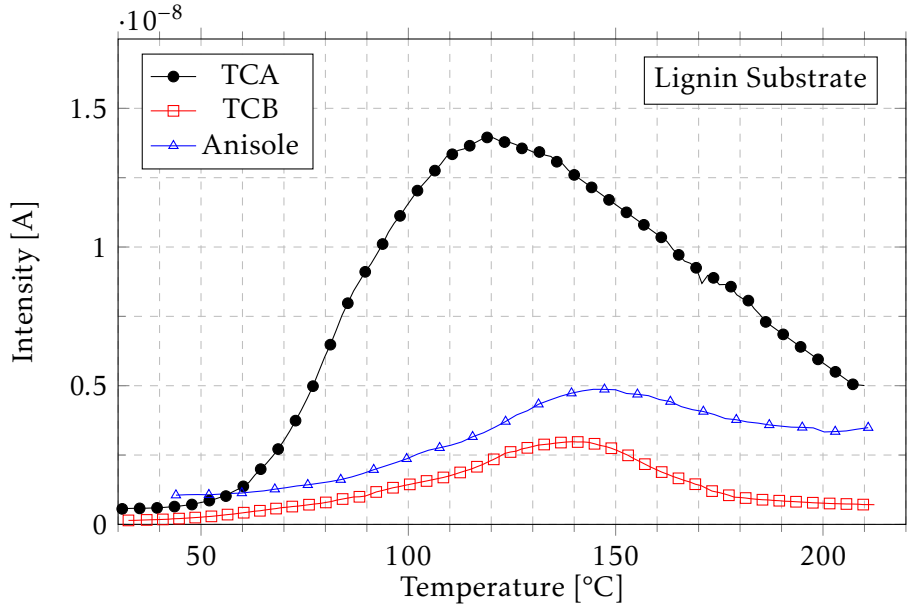

Figure 5.11: Desorption spectra of the different adsorbates while using a lignin substrate.

In the desorption spectra represented in this figure, there is only one peak instead of the usual two, that were previously observed in figure 5.10, with a cork substrate. Considering the large FWHM in the TCA and in anisole spectrum, it is very likely that a convolution is covering the presence of other desorption peaks.

The peaks are not so clear in a lignin substrate with their FWHM ranging from 50ºC in TCB to almost 120ºC in TCA.

Regarding the anisole spectrum, it is not clear whether it continues towards higher temperatures or not. However, considering that the intensity at this temperature is approximately the same as in its desorption peak at 144°C, it seems that there would be other peaks beyond 200°C.

Concerning the position and the shape of each desorption peak, there is a clear difference in the spectra, by changing from a cork substrate to a lignin substrate. Besides the decrease in the number of desorption peaks, the temperatures of the peak's maximum desorption rate in a lignin substrate are below the temperatures that were observed in the desorption spectra from the cork substrates. For TCA, the maximum desorption rate

occurs at 119ºC,for TCB at 140°C and for anisole at 144°C. The decrease in the temperature at which the peak is positioned indicates that the adsorbates establish a weaker bond with lignin than they establish with cork subtrates.

The desorption energies for the contaminants in a lignin substrate, according to Redhead's method, are 113.6 kJ/mol for TCA, 119.5 kJ/mol for TCB and 120.7 kJ/mol for anisole.

In figure 5.12, the substrate was changed to another cork component, cellulose. Similarly to lignin, the desorption spectra of each contaminant in a cellulose substrate only has one desorption peak. The TCA spectra has the most prominent peak in this figure, with a maximum at 90ºC. It is also possible to see in the desorption spectra a shoulder-type peak at 108.2ºC. TCB and anisole are not as clearly shaped as the TCA curve, having their maximum desorption rate close to each other at 110ºC and 102ºC, respectively.

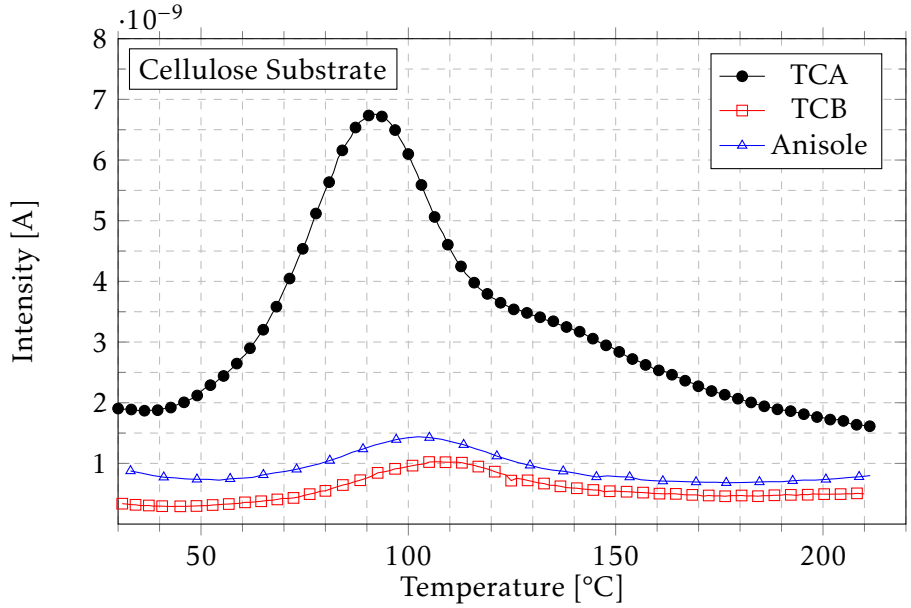

Figure 5.12: Desorption spectra of the different adsorbates while using a cellulose substrate.

Comparing lignin spectra, in figure 5.11, with cellulose desorption spectra in figure 5.12, the only similarity found is the number of peaks each spectrum has. However, comparing with figure 5.10, which has a cork substrate, it is possible to see that the lower temperature peak on both spectra are a match. In the cork substrate this peak is at a temperature of 86°C and in the cellulose substrate is at a temperature of 90°C.

The peaks in cellulose desorption spectra are better defined but, considering the spectra intensities, the species seem to adsorb less in cellulose substrates than with any other substrate. This may be related with its structure. For example, opposed to cork, cellulose does not have any cells or any lenticular channels in which the contaminants could easily adsorb.

The desorption energies for the determined peaks are 104.7 kJ/mol and 118.4 kJ/mol

(considering the shoulder-type peak) for TCA, 110-6 kJ/mol for TCB and 108.2 kJ/mol for anisole.

5.5 Desorption of TCA-like molecules

In this section, a different comparison and analysis is done from a different perspective to understand how the adsorbates desorb from the surface of the different substrates. The spectra are thus grouped by the adsorbate used in the TPD experiments, instead of being grouped by the substrate used.

Considering the TCA spectra, figure 5.13, it is possible to notice that the peaks at a temperature close to 90°C seem to match. The desorption peak from a cork substrate is at 86°C and the desorption peak from the cellulose substrate is at 90°C. The second peak of TCA, which is at 160ºC, has no correspondent peak in any of the other substrates peaks.

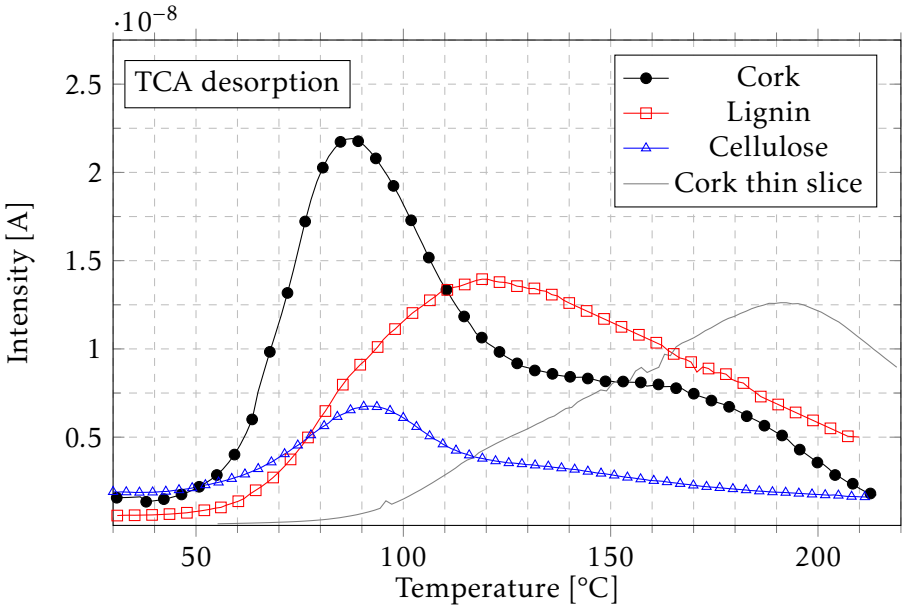

Figure 5.13: TCA desorption spectra from the different substrates used.

On the one hand, TCA establishes the weakest bond with cellulose. It has a low temperature peak and comparing qualitatively the intensities, cellulose also has the lowest intensity through the whole temperature sweep. On the other hand, both cork and lignin seem to be good substrates for TCA adsorption since both have a relatively high temperature desorption peak in cork and a high temperature desorption peak in a lignin substrate. The amount of contaminant removed, however, seems to be distributed throughout the whole temperature sweep in a lignin substrate, while in this particular case of a cork substrate, most of TCA was removed in the lower temperature peak.

In this figure is also showed the desorption spectra of TCA from a thin slice of cork. The experimental conditions for the acquisition of this spectra were practically the same

and the heating rate used was of 5ºC/min as well. However, the pressure observed throughout the experiment was slightly inferior to what was observed with the thicker slices. This is easily explained by the thickness reduction. By decreasing the thickness of the substrate, it has less surface for water vapour or for any other species to adsorb on it. Thus, when realizing a TPD experiment the pressure should be inferior to what was observed with the thicker slices. Notice that the higher temperature peak of TCA desorption spectrum shifted to even higher temperatures in the thinner substrate desorption spectrum. While that peak was still present in the desorption spectrum of the thinner slice, the lower temperature peak was removed, supposedly, with the thickness change. Considering the peak's maximum desorption rate, it seems that TCA established a stronger bond with the thin slice than with the thicker slice. While in the thick slice, the desorption energy was of 126.1 kJ/mol, in the thin slice the desorption energy was of 133.9 kJ/mol.

In figure 5.14, are grouped the three desorption spectra of trichlorobenzene for each substrate used. In this case, there is a great difference in intensities. This contaminant seems to be less detected while desorbing from other substrates that are not cork. Furthermore, in the TCB desorptions, opposed to what was observed in the TCA spectra in figure 5.13, there are not any obvious similarities nor desorption peaks matching in temperature.

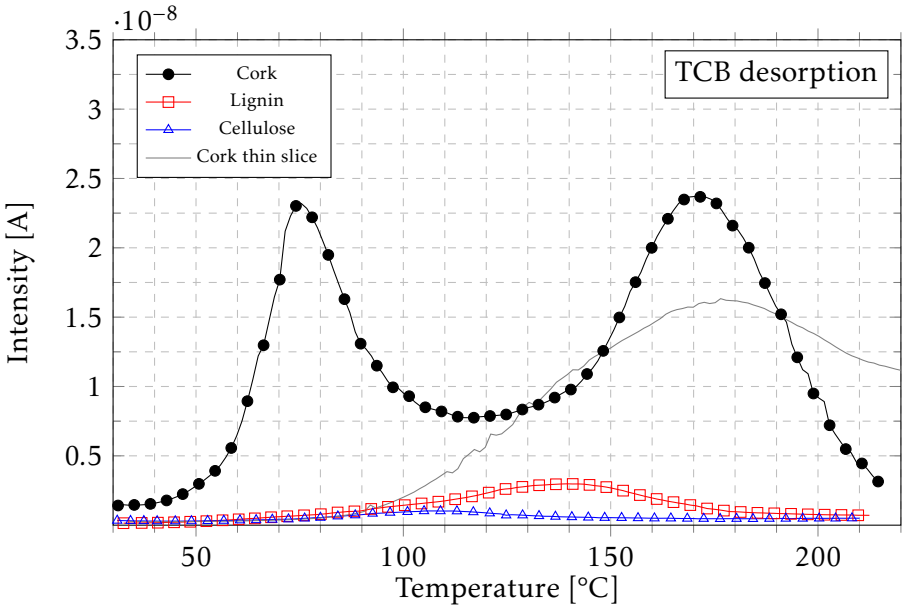

Figure 5.14: TCB desorption spectra from the different substrates used.

Similarly to the experiment described in figure 5.13 a thin slice of cork was tested under the same conditions. Its desorption spectra has a higher temperature peak which comparing with the TCB desorption spectra in a cork substrate did not significantly change its maximum position, which only changed from 170ºC to 176ºC. It seems that it had its intensity lowered at the cost of an increase in the FWHM. As it happened with the

TCA spectra of the thin slice of cork previously observed in this subsection (figure 5.13), the lower temperature peak is not seen in the desorption spectra of TCA from the thin slice of cork. Also worth noting is how high the intensity of the spectrum is, comparatively with the peak's maximum desorption rate, at temperatures above 200ºC. It seems that there may be another desorption peak present or convoluted, in higher temperatures.

Regarding desorption energies in the cork substrates and considering the most energetic peaks, they are practically the same with 128.5 kJ/mol, for the thicker slice, and 130.3 kJ/mol in the thinner slice.

The desorption spectra of anisole (figure 5.15) seems to have a peak in the cork substrate desorption spectrum that is almost matching with the peak in the cellulose substrate. We are, however, comparing a shoulder-type peak of the anisole spectra in a cork substrate with the absolute maximum of anisole desorption spectra, in a cellulose substrate. As already mentioned before, the shoulder peak position in cork is at 96ºC and in cellulose is at 102ºC, meaning that the maximum of each peak differ by 6ºC which translates into a difference of almost 2 kJ/mol, in the desorption energies.

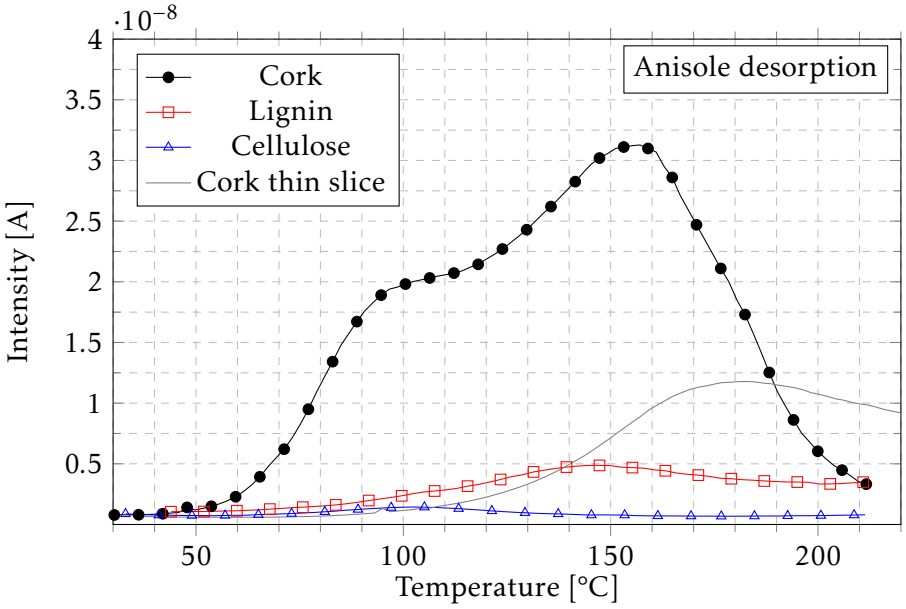

Figure 5.15: Anisole desorption spectra from the different substrates used.

The higher temperature peaks from the cork and from lignin substrate are approximately at the same temperature, with the maximum of each peak being at 157ºC, in cork, and at 144ºC, in lignin. However they are not a perfect match.

Regarding the cork substrates, the thin slice of cork has a high temperature peak that went through a shift of 26°C, towards higher temperatures, changing from 157°C to 183°C. Comparing intensities qualitatively, it seems that the intensity of this peak had decreased. Again, this decrease could possibly be explained by the lower surface are in a thinner slice for the molecules to adsorb. Notice that the thin slice, as it happened with the TCA spectra, had its peak position shifted to higher temperatures, meaning that

even though the slice is thinner, the adsorption established holds more energy than the adsorption in the thick slice.

The desorption energies of anisole in the cork substrates increased from 124.9 kJ/mol to 132.7 kJ/mol, with the thickness change.

Chapter 6

Conclusion

The intended goals for this thesis were to understand how the adsorption and desorption of TCA onto cork substrates occurred. Considering the work done in this thesis and the objectives initially defined, it is possible to take some conclusions towards the desorption of 2,4,6-trichloroanisole (TCA) from cork substrates.

Using temperature-programmed desorption combined with quadrupole mass spectrometry, it was observed that TCA desorbed from cork substrates. Since the mass spectrometer has limitations, regarding the detection of TCA within concentrations that the human senses can easily detect, the substrates had to be well contaminated. Therefore, an amount of 400 μg of TCA was used to obtain its desorption spectra on cork. The maximum desorption rate of this peak is at a temperature of 162°C and was obtained under vacuum conditions. A heating rate may be used in the TPD experiment, however it is not essential to desorb the TCA molecules from the surface of the substrate.

The main outcome of this experiment is that by exposing a substrate contaminated with TCA to a temperature above the maximum desorption rate of the TCA desorption spectrum (162°C) it is possible to desorb TCA from cork substrates.

The quantification method implemented in this thesis work allowed to take another conclusion. By being able to quantify the TCA that is desorbed from cork substrates, it was possible to compare the amount of TCA used in the contamination of the substrates with the amount of TCA that desorbed from the substrate. This method determined that these amounts of TCA are within the same range. Therefore, in the identified desorption peak of TCA, at a temperature of 162°C, the majority of TCA is removed. If any desorption peaks are to be found in temperatures above 220°C, the contributions are negligible.

In the experiments in which the samples were heated pre-TPD, the contaminated substrates were heated to 50ºC, while in the other experiment the substrates were not heated pre-TPD. The desorption spectra of the non-heated contaminated substrates consisted of

two peaks, one at 64°C and another at 158°C. With this experiment, we verified that the lower temperature peak was absent in the desorption spectra of the pre-heated substrates. This was consistent throughout the desorption spectra done in this experiment.

The absence of the desorption peak could mean one of two situations:

- The TCA detected in the lower temperature peak is released to the gas phase, by heating, and is removed by the pumping system;
- The TCA detected in the lower temperature peak is desorbed and re-adsorbed at higher adsorption energies, which is desorbed again when overcoming a temperature of approximately 160ºC.

However, even though the integral value was relatively close, it is still uncertain which option corresponds to the reality.

Regarding the clean cork experiment, it was noticed that the hydrocarbons have relevant contributions in the background desorption spectra.

Different adsorbates and substrates, related to the chemical structure of TCA and to the constitution of cork, were tested. In this experiment, it was noticed that the TCB desorption spectra was different than expected. Since the molecule of TCB has three chlorine atoms, similarly to the molecule of TCA, the hypothesis was that these three chlorine atoms were contributing to the adsorption of TCA. Therefore, it should be expectable to find a similar desorption spectrum to the TCA spectra previously obtained. However it is possible that that is not the case since the experiments done with the chlorinated adsorbates, concerning the three chlorine atoms hypothesis, were inconclusive.

Considering the spectra obtained for either TCB or anisole spectra, it is not possible to precisely compare intensities regarding these two contaminants, since there is not a reference leak for these adsorbates. However, it is possible to qualitatively compare the intensities of these spectra and thus it is possible to state that the intensities of desorption spectra of the chosen adsorbates are within the same magnitude. The desorption spectra of the adsorbates from a cellulose substrate seem to be an exception, being one order of magnitude below its typical values. This means that the adsorption on cellulose holds less energy, than the adsorption on a substrate of cork or lignin. Consequently it is not as relevant for the TCA adsorption on cork substrates as, for instance, lignin.

A reduction of the thickness of cork substrates was also experimented. The substrates which were tested had a thickness of 1 mm. By reducing the thickness of the cork substrates, we had the purpose of observing as much as possible the desorbed TCA that comes from the surface of the cork. Later, and still considering this purpose, it was also tested spray contaminations of the substrates, so these contaminations were as superficial as possible. Neither experiments brought any obvious answers to the many questions already pointed. Although, the spectra for the different contaminants seem to share some similarities. These spectra have one large desorption peak, which could be a convolution

of several lesser peaks, and have their maximum desorption rate relatively close to a temperature of 180ºC, differing by 8ºC at the most.

Making a comparison between the desorption spectra before and after the thickness change, it is possible to notice the absence of the lower temperature peak from the spectra. This peak may resemble the earlier pre-heating experiments, where the low temperature peak was removed after pre-heating the substrates to 50°C. Also worth noting is the fact that in the thinner slices the adsorbates seem to establish a stronger bond with the substrate. This is easily noticed when observing the position of the peak at higher temperatures.

Nonetheless, two important conclusions were done. One of the main contributions of this thesis work was the confirmation that TCA is removed from cork substrates, when heating the contaminated substrates above a temperature of 160°C, under vacuum. Another conclusion was that by using the quantification method developed, it was possible to determine that the removed TCA is in the range of the initial amount of adsorbate used to contaminate the substrates, confirming the efficiency of this desorption process.

6.1 Future Work

Following this thesis work and in order to understand how TCA adsorbs and desorbs from cork, some improvements should be considered and new objectives should be traced.

Suberin is the most abundant material in the constitution of cork. Thus, its contribution may be relevant towards the understanding of TCA adsorption on cork substrates. Therefore, it should be tested and used as a substrate in the near future.

Using the same piece of cork as substrate in the same type of experiments should also be a situation to be tested. However, the integrity of these samples should be carefully verified between each TPD.

Besides the substrates, if the contaminants are to be reconsidered and changed, it should be towards knowing how the number of chlorine atoms contribute to the adsorption of chlorinated compounds, such as TCA, TCB or even different adsorbates such as dichlorobenzene or tetrachlorobenzene.

Regarding the experimental set-up and the sections defined, more reference leaks should be installed. At the moment, the system is limited to the TCA reference leak. However, if different references were used, for instance for TCB, anisole or any other contaminant, that could lead into some conclusions which could help trace different objectives.

The spray contaminations were introduced in the final stage of this thesis work and, thus, this procedure still has margin for improvements. These improvements should be done while taking into account some considerations, such as knowing how much adsorbate is sprayed onto the samples or if the adsorbate is equally distributed through the substrate surface.

Another alternative method of substrate exposure to the adsorbates would consist in having the substrates in the top of a chamber and then, by having one surface of the substrate exposed to a gas, the adsorption would occur.

Besides the changes in the experimental procedures that should be done in future experiments, an alternative desorption process should be considered. This process is illustrated in figure 6.1.

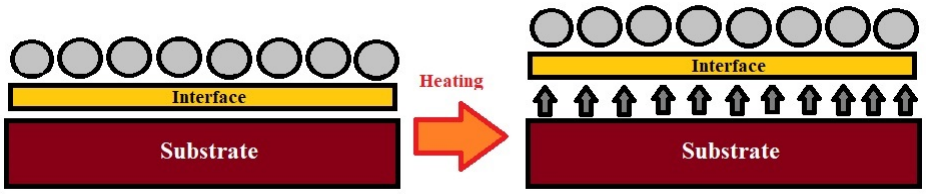

Figure 6.1: Illustration of a possible alternative desorption process.

This desorption process consists, for instance on TCA adsorbing to a cork's extractive and then, by heating, desorb the extractive along with the adsorbate from the substrate, instead of desorbing the adsorbate directly from the substrate.

Nonetheless, since in this case it is worth having a vacuum system that has a working pressure as low as possible, a trap could be strategically set between the entrance of the main chamber and the sample insertion section, in order to improve the working pressure.

Bibliography

[1] H. R. Buser, C. Zanier, and H. Tanner. "Identification of 2,4,6-trichloroanisole as a potent compound causing cork taint in wine." In: *Journal of Agricultural and Food Chemistry* 30.2 (1982), pp. 359–362. ISSN: 0021-8561. DOI: 10.1021/jf00110a037. URL: http://pubs.acs.org/doi/abs/10.1021/jf00110a037.

[2] D. L. Capone, G. K. Skouroumounis, and M. a. Sefton. "Permeation of 2,4,6-trichloroanisole through cork closures in wine bottles." In: *Australian journal of grape and wine research* 8.3 (2002), pp. 196–199. ISSN: 1322-7130. DOI: 10.1111/j.1755-0238.2002.tb00256.x. URL: http://doi.wiley.com/10.1111/j.1755-0238.2002.tb00256.x.

[3] E. Herve, S. Price, G. Burns, and P. Weber. "Chemical Analysis of TCA As a Quality Control Tool For Natural Corks." In: (2006), p. 16.

[4] Cork Supply. *Innocork - Cork Supply*. URL: https://www.corksupply.pt/pt/compromisso-de-qualidade/innocork/ (visited on 09/01/2017).

[5] T. J. Evans, E. Butzke, and S. E. Ebeler. "Analysis of 2,4,6-trichloroanisole in wines using solid-phase microextraction coupled to gas chromatography-mass spectrometry." In: *Journal of Chromatography A* (1997).

[6] S. Corp. "Determination of 2,4,6-trichloroanisole in Wine with SPME and the 4000 GC/MS." In: *Varian* i (2010), pp. 1–6. DOI: 10.1016/B978-0-12-373628-4.00043-5.

[7] I. Márquez-Sillero, E. Aguilera-Herrador, S. Cárdenas, and M. Valcárcel. "Determination of 2,4,6-tricholoroanisole in water and wine samples by ionic liquid-based single-drop microextraction and ion mobility spectrometry." In: *Analytica Chimica Acta* 702.2 (2011), pp. 199–204. ISSN: 00032670. DOI: 10.1016/j.aca.2011.06.046.

[8] A. R. Fontana, S. H. Patil, K. Banerjee, and J. C. Altamirano. "Ultrasound-assisted emulsification microextraction for determination of 2,4,6-trichloroanisole in wine samples by gas chromatography tandem mass spectrometry." In: *Journal of Agricultural and Food Chemistry* 58.8 (2010), pp. 4576–4581. ISSN: 00218561. DOI: 10.1021/jf904396g.

[9] V. Varelas, N. Sanvicens, M-Pilar-Marco, and S. Kintzios. "Development of a cellular biosensor for the detection of 2,4,6-trichloroanisole (TCA)." In: *Talanta* 84.3 (2011), pp. 936–940. ISSN: 00399140. DOI: 10.1016/j.talanta.2011.02.029. URL: http://dx.doi.org/10.1016/j.talanta.2011.02.029.

[10] Amorim Cork. *Bark To Bottle*. 2016.

[11] M. K. Taylor, T. M. Young, C. E. Butzke, and S. E. Ebeler. "Supercritical fluid extraction of 2,4,6-trichloroanisole from cork stoppers." In: *Journal of Agricultural and Food Chemistry* 48.6 (2000), pp. 2208–2211. ISSN: 00218561. DOI: 10.1021/jf991045q.

[12] N. Park, Y. Lee, S. Lee, and J. Cho. "Removal of taste and odor model compound (2,4,6-trichloroanisole) by tight ultrafiltration membranes." In: *Desalination* 212.1-3 (2007), pp. 28–36. ISSN: 00119164. DOI: 10.1016/j.desal.2006.10.002.

[13] J. P. Obrech. *Cork stopper decontamination device*. 2006.

[14] P. Vlachos, A. Kampioti, M. Kornaros, and G. Lyberatos. "Development and evaluation of alternative processes for sterilization and deodorization of cork barks and natural cork stoppers." In: *European Food Research and Technology* 225.5-6 (2007), pp. 653–663. ISSN: 14382377. DOI: 10.1007/s00217-006-0461-3.

[15] P. Vlachos, E. Stathatos, G. Lyberatos, and P. Lianos. "Gas-phase photocatalytic degradation of 2,4,6-trichloroanisole in the presence of a nanocrystalline Titania film. Applications to the treatment of cork stoppers." In: *Catalysis Communications* 9.10 (2008), pp. 1987–1990. ISSN: 15667367. DOI: 10.1016/j.catcom.2008.03.031.

[16] M Careri, V Mazzoleni, M Musci, and R Molteni. "Study of Electron Beam Irradiation Effects on 2,4,6-Trichloroanisole as a Contaminant of Cork by Gas Chromatography-Mass Spectrometry." In: *Chromatographia* 53.9 (2001), pp. 553–557. ISSN: 00095893. DOI: 10.1007/BF02491621.

[17] C. Pereira, L. Gil, and L. Carriço. "Reduction of the 2,4,6-trichloroanisole content in cork stoppers using gamma radiation." In: *Radiation Physics and Chemistry* 76.4 (2007), pp. 729–732. ISSN: 0969806X. DOI: 10.1016/j.radphyschem.2006.04.002.

[18] K Jousten. *Handbook of Vacuum Technology*. 2nd. Vol. 24. 2008, p. 1040. ISBN: 3527407235. DOI: 10.1002/9783527688265. URL: https://books.google.com/books?id=Gco{_}ytUu4QYC{\&}pgis=1.

[19] S. Schroeder and M Gottfried. "Temperature-Programmed Desorption (TPD) Thermal Desorption Spectroscopy (TDS)." In: *Userpage.Chemie.Fu-Berlin.De* June (2002), pp. 1–22. ISSN: 00396028. DOI: http://www.chemie.fu-berlin.de/~pcprakt/tds.pdf. URL: http://scholar.google.com/scholar?hl=en{\&}btnG=

Search{\&}q=intitle:Temperature-Programmed+Desorption+(TPD)+Thermal+Desorption+Spectroscopy+(TDS){\#}7.

[20] T. ALTHERR. "Introduction To Thermal Field Theory." In: *International Journal of Modern Physics A* 08.32 (1993), pp. 5605–5628. ISSN: 0217-751X. DOI: 10.1142/S0217751X93002216. arXiv: 9307277 [hep-ph]. URL: http://www.worldscientific.com/doi/abs/10.1142/S0217751X93002216.

[21] T. Ishii and T. Kyotani. *Temperature Programmed Desorption*. 2016, pp. 287–305. DOI: 10.1016/B978-0-12-805256-3.00014-3. URL: http://linkinghub.elsevier.com/retrieve/pii/B9780128052563000143.

[22] P. Redhead. "Thermal desorption of gases." In: *Vacuum* 12.4 (1962), pp. 203–211. ISSN: 0042207X. DOI: 10.1016/0042-207X(62)90978-8. URL: http://linkinghub.elsevier.com/retrieve/pii/0042207X62909788.

[23] FHI. "Desorption techniques." In: *FHI Vorlesung TPD. Lecture*. 2006.

[24] G. B. Cooke. "Cork and the cork tree." In: (1961), p. 121.

[25] H. Pereira. *Cork : biology, production and uses*. 2007, p. 336. ISBN: 9780444529671.

[26] H. Pereira. "Chemical composition and variability of cork from Quercus suber L." In: *Wood Science and Technology* 22.3 (1988), pp. 211–218. ISSN: 00437719. DOI: 10.1007/BF00386015.

[27] J. Graça and H. Pereira. "Cork Suberin: A Glyceryl Based Polyester." In: *Holzforschung* 51.January (1997), pp. 225–234. ISSN: 0018-3830. DOI: 10.1515/hfsg.1997.51.3.225.

[28] H. Rudy. "Efficient and sensitive determination of TCA and other off-flavors." In: *Gerstel* 11 (), pp. 9–11.

[29] C. Macku and K. Reed. *Factors affecting wine closure selection*. 2011. URL: https://www.practicalwinery.com/winter2011/closure3.htm (visited on 07/20/2008).

[30] R. F. Simpson and M. Sefton. "Origin and fate of 2,4,6-trichloroanisole in cork bark and wine corks." In: *Australian Journal of Grape and Wine Research* 13.2 (2007), pp. 106–116. ISSN: 13227130. DOI: 10.1111/j.1755-0238.2007.tb00241.x.

[31] NIST. *2,4,6-trichloroanisole Mass Spectrum*. 2017. URL: http://webbook.nist.gov/cgi/cbook.cgi?ID=C87401{\&}Mask=200{\#}Mass-Spec (visited on 09/01/2017).

[32] NIST. *1,3,5-trichlobenzene Mass Spectrum*. 2017. URL: http://webbook.nist.gov/cgi/inchi?ID=C108703&Mask=200#Mass-Spec (visited on 09/01/2017).

[33] NIST. *Anisole Mass Spectrum*. 2017. URL: http://webbook.nist.gov/cgi/cbook.cgi?ID=C100663&Mask=200#Mass-Spec (visited on 09/01/2017).

[34] NIST. *Hexadecane Mass Spectrum*. URL: http://webbook.nist.gov/cgi/cbook.cgi?ID=C544763{\&}Units=SI{\&}Mask=2FF{\#}Mass-Spec (visited on 09/01/2017).

Appendix

Desorption Results

Table A.1: Table of desorption energies that were indicated in chapter 5 of this document.

Figure	Contaminant	Substrate	Acquisition Date	T_p	β	Edes [kJ/mol]
5.3	-	Cork Thick Slice	22-05-2017	-	1	-
-	-	Cork Thin Slice	-	-	1	-
5.5	TCA	Cork	30-03-2017	162	1	131.9
5.6	TCA	Cork	28-03-2017	64	1	101.5
-	-	-	-	158	-	130.7
5.7.a	TCA	Cork	07-04-2017	74	1	104.6
-	-	-	-	164	-	132.5
-	-	-	07-04-2017	162		131.9
5.7.b	-	-	10-04-2017	76	1	105.2
-	-	-	-	164	-	132.5
-	-	-	10-04-2017	156	-	130.1
5.7.c	-	-	11-04-2017	76	1	105.2
-	-	-	-	162	-	131.9
-	-	-	11-04-2017	162	-	131.9
5.7.d	-	-	20-04-2017	80	1	106.4
-	-	-	-	174	-	135.7
-	-	-	20-04-2017	166	-	133.2
5.7.e	-	-	24-04-2017	80	1	106.4
-	-	-	-	164	-	132.5
-	-	-	26-04-2017	160	-	131.3
5.8	Teflon	Cork	05-04-2017	-	1	-
5.9	TCA	Cork	18-04-2017	86	1	103.5
-	-	-	-	162	-	131.9
5.10	TCA	Cork	08-06-2017	86	5	103.5
-	-	-	-	161	-	126.1
-	TCB	-	08-06-2017	75	-	100.5
-	-	-	-	170	-	128.5
-	Anisole	-	08-06-2017	96	-	106.5
-		-	-	157	-	124.9
5.11	TCA	Lignin	07-06-2017	119	5	113.6
-	TCB	-	07-06-2017	140	-	119.5
-	Anisole	-	07-06-2017	144	-	120.7
5.12	TCA	Cellulose	05-06-2017	90	5	104.7
	-	-	-	136	-	118.4
	TCB	-	05-06-2017	110	-	110.6
	Anisole	-	05-06-2017	102	-	108.2
			Thin Slices			
5.13	TCA	Cork	19-06-2017	188	5	133.9
5.14	TCB	Cork	16-06-2017	176	-	130.3
5.15	Anisole	Cork	16-06-2017	183	-	132.7